Addis Ababa University

Addis Ababa Institute of Technology

School of Multidisciplinary Engineering

Center for Materials Engineering

Enhancing the Catalytic performance of CuS for C_{2+} products from CO_2 Reduction via Zn Doping, Vacancy Defects and Facet Engineering

By

Meseret Kebede Demisse

This Thesis is Submitted to Center for Materials Engineering, Addis Ababa Institute of Technology, Addis Ababa University in Partial Fulfillment of the Requirements for the Degree of Master of Science in Materials Engineering

Advisor: ***Georgis Alene (Dr)***

March, 2025

Addis Ababa, Ethiopia

Confirmation Page

The thesis by Meseret Kebede, entitled " ***Enhancing the Catalytic performance of CuS for C_{2+} products from CO_2 Reduction via Zn Doping, Vacancy Defects and Facet Engineering*** *" for the master of science in materials engineering degree, has been certified to meet university regulations and standards for originality and quality.*

Approval by the Board of Examiners

	Signature	*Date*
Georgis Alene (Dr)	_____	_____
Advisor		
Kefale Wagaw (Dr)	_____	_____
Co. Advisor		
Kingsly Obodo(Dr)	_____	_____
Co. Advisor		
Tesfaye Refera (Dr)	_____	_____
Internal Examiner		
Aman Kasa (Dr)	_____	_____
External Examiner		

DECLARATION

I can confirm that this thesis is completely original and hasn't been submitted before for credit towards any degree at any college. All the sources I've used for this thesis have been properly cited.

Name: Meseret Kebede

Signature: _____

To the best of our knowledge, we hereby certify that the candidate's declaration is accurate and has been submitted for the examination with our approval as university advisors.

Goergis Alene Asres (Dr)	signature	Date
Advisor	_____	_____

Date of submission: March, 2025

Table of Contents

List of Figures

List of Tables

List of Acronym

C2H4	ethylene
C2H6	ethane
CH_3COOH	acetic acid
C_2H_5OH	ethanol
CO	Carbon mono oxide
CO_2	Carbon dioxide
CO2RR	carbon dioxide reduction reaction
Cucub	Copper cube
Cuoh	Copper octahedron
CuS	Copper Sulfid
Cusph	Copper sphere
DFT	Density functional theory
ERC	electro chemical reduction of carbon dioxide
ESPRESSO	opEn-Source Package for Research in Electronic Structure, Simulation, and Optimization
GGA	General Gradient Approximation
HCOOH	formic acid
HER	Hydrogen evolution reaction
MS	Materials Studio
n-CuNS	nanodefective Cu nanosheet
PBE	Perdew–Burke– Ernzerh
VKS	Kohn-Sham potential
XCrySDen	Crystalline Structures and Densities

Acknowledgment

First and foremost, I want to express my deepest gratitude to God Almighty and His Mother, Saint Virgin Mary, for giving me the opportunity, the strength, and the courage to keep learning, and for everything that has happened in my whole life. Following God, I wish to extend our sincere appreciation to the Addis Ababa Institute of Technology for providing women with this invaluable scholarship opportunity.

I would also like to convey my heartfelt thanks to my advisor, Dr. Georgies Alene, for his steadfast support, encouragement, patience, and extensive knowledge. His guidance and insightful feedback have been immensely beneficial throughout the entire thesis writing process.

I am immensely appreciative of my co-advisor, Dr. Kefale Wagaw, for his essential support. He patiently shared his research methods with me, encouraged me, corrected my errors, and taught me a lot. In addition, I would like to express my gratitude to Dr. Kingsley Obodo he also my co. advisor. Who provides the essential resources such as allowing me to use the South African supercomputer, which enabled Quantum Espresso. and ongoing support; without which I could not have finished this thesis.

I would like to thank everyone of the staff at the Center for Material Engineering (CME) for their assistance and encouragement during my thesis research.

I also want to express my gratitude to my family for their constant support and encouragement during this entire research process.

Abstract

Through doping, defect engineering, and facet engineering, this study explores methods to improve the catalytic performance of copper sulfide (CuS) for the electrochemical reduction of carbon dioxide (CO_2) into C_{2+} products. We examine the impact of different changes on the electronic structure and catalytic activity of CuS using density functional theory (DFT) simulations. To maximize active sites for CO_2 adsorption and conversion, facet engineering, zinc (Zn) doping and creating Cu vacancies in the CuS structure are being investigated. As per the study, certain configurations on the CuS(110) surface, like the End-on and Side-on orientations, show significantly lower adsorption energies, suggesting more advantageous reaction pathways for CO_2 reduction. The results demonstrate that Zn-doped CuS(110) surface both one Cu replaced by one Zn and one S replaced by one Zn and Cu vacancy sites on CuS(110) surface End-on for the surface physio and Side-on for the Surface physio orientations, show significantly lower adsorption energies, suggesting more advantageous reaction pathways for CO_2 reduction and change the CO_2RR performance of Cu-based catalysts and enhance catalytic activity by simplifying CO_2 activation and improving selectivity for C_{2+} products. So from this result End-on for the surface physio and Side-on for the Surface physio orientations or active site is preferable for carbon dioxide reduction reaction. Additionally, it is shown that facet engineering is important in determining the reactivity of CuS, with some facets outperforming others. This work provides crucial insights into the design of efficient CuS-based catalysts for CO_2 conversion, highlighting the potential for structural changes to result in enhanced catalytic efficiency and selectivity in sustainable energy applications.

CHAPTER ONE

1. Introduction

1.1. Background of The Study

Carbon dioxide (CO_2) levels in the atmosphere are rising due to industrial processes and the burning of fossil fuels, which poses a serious threat to the stability of the global climate. Since CO_2 is a powerful greenhouse gas that contributes to climate change and global warming, it is essential to implement immediate and workable solutions[1][2][3]. Currently, gigatons of carbon are released into the atmosphere annually from the combustion of fossil fuels. Consequently, From 1850 to 1975, human activities have increased the amount of atmospheric CO_2 from 290 ppm to more than 330 ppm, and as of 2018, more than 407 ppm [4]. Converting CO_2 into useful chemical feedstocks and fuels, especially C_{2+} products like ethylene, ethanol, and other hydrocarbons, is a promising strategy to address this environmental issue. This not only lowers CO_2 levels in the atmosphere but also offers a sustainable way to produce necessary chemicals[5][6] .

Thermochemical, photochemical, and electrochemical technologies, among others, are intriguing for converting CO_2 into industrial chemicals and fuels. Among these methods, electrochemical reduction of CO_2 (ERC) reaction is a potential technology for turning waste CO_2 into fuels and feedstock is seen as an attractive strategy that is safe and inexpensive as it is a process that can contribute to the mitigation of climate change [7]. Electrochemical reduction is a promising method for converting CO_2 into value-added products such as formic acid (HCOOH), carbon monoxide (CO), acetic acid (CH_3COOH), ethylene (C_2H_4), ethane (C_2H_6), ethanol (C_2H_5OH), and other hydrocarbons, while also improving the energy crisis and lowering global carbon emissions. With the advantages of being driven by renewable electricity, good controllability, mild reaction conditions, and high energy density of the delivered products, CO_2RR has increased widespread interest for CO_2 conversion [8].

Out of all the different catalytic systems that have been studied for reducing CO_2, copper-based catalysts, particularly CuS, have become the preferred choice. This is because Copper sulfide (CuS) really shines when compared to other copper catalysts like metallic copper (Cu) and copper

oxide (CuO), especially when it comes to using electricity to turn carbon dioxide (CO_2) into useful products. CuS's big advantage is its special talent for making bigger hydrocarbon molecules, particularly C_{2+} ones like ethylene and ethanol, which are worth more money. On the flip side, Cu usually just makes smaller C_1 products like methane and formic acid, and CuO isn't as good at the whole reduction process. The electrically adjustable properties, affordable price, and wide availability of CuS catalysts make them particularly attractive[9]. While there is much promise for CuS, it typically fails to convert CO_2 into something beneficial in practical applications. Low selectivity, which means it doesn't always pick the product we want, insufficient activity, which means it doesn't always pick the product we want, and stability issues, which means it can break down over time while being used, are caused by its propensity to struggle with these three main issues. For large-scale CO_2 conversion, CuS is challenging due to these problems[10][11].

Researchers have adopted cutting-edge methods centered on modifying the catalyst's makeup and characteristics to augment the catalytic efficacy of CuS. In recent years, three prominent approaches—facet engineering, defect engineering, and doping—have drawn heightened interest. Each method provides a distinct pathway to elevating the potency and efficiency of CuS catalysts in CO_2 transformation[12].

Doping is the deliberate addition of foreign atoms to the CuS structure. This modification may significantly alter the electronic properties of the catalyst, potentially improving the reaction kinetics and selectivity of the C_{2+} product. Researchers can meticulously choose dopants to precisely adjust the electronic properties of CuS. CuS doped with zinc (Zn) has shown promise in enhancing its conductivity and catalytic activity. Specifically, this approach can modify the band structure, potentially improving charge carrier density and conductivity, which are crucial for electrochemical reactions [13]. Because of Zn is ecofriendly, cost effective, corrosion resistance catalytically reactive with Copper [14].

Defect engineering is a smart strategy to enhance the effectiveness of CuS catalysts. This method deliberately introduces structural flaws, such as vacancies, into the catalyst's structure. Although these imperfections might seem unwanted, they are actually quite advantageous. These strategically created defects serve as powerful catalytic active sites. Through the incorporation of

these calculated flaws, we're able to enhance the way reactants and intermediates bind, effectively guiding the reactions more smoothly towards the desired outcomes. Consequently, this boosts the catalyst's overall effectiveness. The presence of defects within a catalyst can actually modify its electronic makeup in a manner that enhances its performance. Studies have found that researchers can significantly improve both the selectivity and effectiveness of CuS catalysts used for CO_2 reduction by carefully controlling the types and amounts of defects present[15].

In contrast, facet engineering is about reshaping the crystal form of CuS to reveal specific crystal facets that possess unique catalytic attributes. The electronic structures and atomic arrangements of various facets can differ, which can affect the catalyst's reactivity and selectivity. By fine-tuning how they grow and make these materials, researchers can zero in on high-energy facets that are better at reducing CO_2. This isn't just a boost for catalytic performance; it also gives us a better understanding of the fundamental steps involved in turning CO_2 into something useful[16].

Using something called DFT calculations, this study takes a systematic look at how adding dopants, creating defects, and changing the facet orientation of CuS impacts its ability to catalyze the production of C_{2+} products from CO_2. The findings from this research could pave the way for more sustainable and powerful catalysts for CO_2 conversion, ultimately helping us reach the big goals of carbon neutrality and using renewable resources.

1.2. Statement of the problem and limitation

The increasing amount of carbon dioxide (CO_2) in our air is causing serious environmental problems. Because of this, we really need to find better ways to use catalysts to turn CO_2 into useful products like ethylene and ethanol [6]. Copper sulfide (CuS) has shown promise as a catalyst for this job because it has great electrical properties and is a good catalyst. CuS, though, often has trouble being a truly great catalyst. It can be a little selective about what it reacts with, might be slow in getting the job done, and could fall apart or become less effective over time. To boost CuS's performance, we need to get imaginative. We can try things like adding other elements to it, deliberately creating tiny imperfections in its structure, or fine-tuning which parts of its surface are most active. These fresh approaches are essential for boosting CuS's ability to convert CO_2 into

valuable C_{2+} products[9]. Fundamentally, these methods aim to enhance the performance of catalysts, significantly boosting their capacity to convert CO_2 into valuable C_{2+} products. This improvement is achieved through adjustments to the catalysts' fundamental constituents, optimization of the electrical current, and modification of their intrinsic electronic configuration. The aim is to make the entire process run smoother and be more selective.

However, even with all these possible benefits, there are certainly some obstacles to overcome. Getting the doping levels precisely right and adding the correct number of defects is a delicate operation. Overdoing the doping or introducing too many defects can actually backfire, making the catalyst less stable and less effective. Also, coming up with ways to make catalysts with the shapes and mixes of ingredients you want can be pretty complicated. Scaling up these methods for widespread industrial application might be quite a challenge. To make matters more complicated, it's difficult to predict the interactions between various dopants and defects, potentially resulting in inconsistent catalyst performance. Furthermore, the long-term stability of engineered CuS catalysts under realistic reaction conditions remains a concern, as they may undergo structural changes or deactivation over time. Lastly, the mechanistic understanding of how these modifications influence the reaction pathways for CO_2 conversion to C_{2+} products is still incomplete, necessitating further research to fully elucidate the underlying processes.

1.3. Research gap

Current research on using CuS as a catalyst for CO_2 reduction tends to zero in on its inherent characteristics and overall effectiveness. However, it often misses opportunities to boost performance by making targeted changes, like adding Zn, creating vacancy defects, or fine-tuning specific crystal facets. Although a few studies have looked at these tweaks individually, we're still missing a complete picture of how they interact and work together to supercharge CuS's ability to produce C_{2+} products.

On top of that, it's not entirely clear from existing research how exactly adding zinc (Zn) changes the electronic structure and reactivity of copper sulfide (CuS). We really need some in-depth theoretical studies using density functional theory (DFT) to figure out how zinc impacts the surface

properties, the way charge is transferred, and how it affects the energies involved when CO_2 and other molecules during the reaction interact with the catalyst.

Plus, we haven't fully explored the role of vacancy defects in making more active sites for these catalytic reactions, nor how these defects affect the stability and selectivity of CuS to produce the desired products. We're also lacking a good understanding of how these vacancy defects alter the electronic states and potentially open up new avenues for the reaction to occur.

Finally, it's worth noting that facet engineering is still a relatively unexplored area, especially when it comes to using CuS for CO_2 electroreduction. Different crystal facets might exhibit different levels of reactivity and selectivity, and using DFT calculations to understand these differences could offer crucial insights that help us optimize CuS for better performance.

1.4. Research questions

1. What are the optimal computational parameters (lattice constant, energy cutoff, charge density cutoff, and k-point grid) for accurately modeling the properties of CuS using Quantum Espresso software?
2. How do the geometric configurations and adsorption energies of bulk CuS, defect structures, and pristine slab CuS (110) influence their suitability as functional materials for carbon dioxide reduction?
3. What are the electronic properties of CuS as determined by band structure calculations, and how do these properties relate to its performance in catalyzing carbon dioxide reduction?
4. How does the adsorption energy of CO_2 vary across different active sites on CuS, and what implications do these variations have for the material's effectiveness in CO_2 capture and conversion?
5. What role do defects in the CuS structure play in modifying its electronic properties and catalytic performance for carbon dioxide reduction?

1.5. Objectives

1.5.1. General objectives

This study aims to enhance the catalytic efficiency of CuS for CO_2 electrochemical reduction in to C_{2+} products by investigating the effects of doping, defect formation, and facet engineering using Density functional theory (DFT)

1.5.2. Specific objectives

- To determine the optimal computational parameters (lattice constant, Energy cutoff, charge density cutoff, and k-point grid) for accurate DFT modeling of CuS.
- To analyze the effect of Zn doping and Cu vacancies on CuS structure and electronic properties to enhance CO_2 adsorption and conversion.
- To compute the band structure and density of state (DOS) of CuS to evaluate its conductivity and catalytic efficiency.
- To compare adsorption energy of CO_2 at different active sites on pristine and modified CuS (110) surfaces and identify the most active catalytic sites
- To provide theoretical insights into how doping, defects, and facet engineering influence CO_2 conversion efficiency for future experimental validation.

1.6. Significance of the study

Improving the catalytic performance of copper sulfide (CuS) towards the production of valuable C_{2+} products, addresses critical environmental challenges associated with CO_2 emissions. The innovative approaches of doping, defect engineering, and facet engineering promote the development of more sustainable materials. This study is particularly significant as it aligns with global efforts to mitigate climate change by transforming CO_2, a greenhouse gas, into useful chemicals. Incorporating advanced computational techniques, such as Density Functional Theory (DFT), to explore the electronic and structural properties of CuS will enhance the understanding of the fundamental mechanisms underlying CO_2 reduction.

1.7. Scope of the study

The scope of this research focuses on enhancing the catalytic performance of copper sulfide (CuS) for the conversion of carbon dioxide (CO_2) into valuable C_{2+} products through advanced engineering techniques. The study aims to optimize critical parameters such as lattice constant, energy cutoff, charge density cutoff, and k-point grid to ensure accurate computational modeling. It will investigate the optimized geometry and adsorption energy of bulk CuS, as well as the composition and structural characteristics of defect-engineered and pristine slab CuS (110) structures, identifying suitable functional materials for CO_2 reduction. Additionally, the research will involve performing band structure calculations to understand the electronic properties of CuS, which are essential for its catalytic activity. Furthermore, the study will calculate the adsorption energy of CO_2 at various active sites using Quantum Espresso software, providing insights into the interaction between CO_2 and the engineered CuS surfaces. By addressing these objectives, the research aims to contribute to the development of more efficient catalysts for CO_2 conversion, ultimately supporting efforts to mitigate greenhouse gas emissions and promote sustainable chemical processes. The work is fully computational and no experimental work is conducted.

CHAPTER TWO

2. Literature Review

2.1.Role of DFT in Catalysis Research

Density Functional Theory (DFT) is a quantum mechanical modeling method widely used to investigate the electronic structure of materials. In the context of catalysis, DFT provides insights into the reaction mechanisms, adsorption energies, and electronic properties of catalysts. By employing DFT, researchers can predict how modifications to the structure of CuS—such as doping, defect engineering, and facet optimization—affect its catalytic performance. Theoretical models have been utilized to identify catalysts with higher electro-catalytic activity and selectivity.

2.2. Electrochemical Reactions

Electrochemical reactions occur when electrons move to or from a molecule, atom, or ion at the boundary where an electronic conductor (an electrode, which is where electrons enter or leave) meets an ionic conductor (where ions flow). These reactions involve two main types of half-cell reactions: oxidation and reduction. Reduction specifically refers to the transfer of electrons from the electrode to the molecule, atom, or ion. A cathodic side reaction is hydrogen generation by

Reduction: $H^{+2} + 2e^{-} \rightarrow H_2$ ……2.1

$2H_2O \rightarrow O_2 + 4H^{+} + 4e^{-}$ ....……2.2

In the language of chemistry, adding electrons to a substance is called reduction. Reaction [2.1] is known as a cathodic reaction, and reaction [2.2] is known as an anodic reaction. When reduction takes place at an electrode, we call it a cathode, and the opposite electrode is called an anode [17].

2.3. Fundamentals of Electrochemical CO_2 Reduction

At its core, electrochemical CO_2 reduction is about grasping how we can turn carbon dioxide (CO_2) into useful stuff using electricity. This approach is a big deal in fighting climate change because it transforms CO_2, a major greenhouse gas, into chemicals and fuels we can actually use [18]. This change takes place at the cathode of an electrochemical cell, where dissolved CO_2 picks up

electrons [17]. Choosing the right catalyst is really crucial to get this process to work effectively and get the results you want, and metals like copper (Cu), silver (Ag), gold (Au), plus a variety of transition metal compounds, are commonly used for this job [19]. The entire process of converting CO_2 into something valuable involves a few stages: first, CO_2 latches onto the catalyst's surface, then it gets activated by gaining electrons, forms some intermediate products, and finally, these intermediate products release to give us the final, useful products. The choice of electrolyte, such as aqueous solutions or ionic liquids, and reaction conditions, including temperature, pressure, and applied potential, significantly influence the efficiency and selectivity of CO_2 reduction [20]. CO_2 reduction for vital fuels and chemicals is an appealing, safe, and cost-effective solution. CO_2 can be converted into fuels using a variety of methods, including electrochemical, thermochemical, and photochemical. Among these techniques to reduce CO_2 emissions from the usage of fossil fuels, the electrochemical conversion of CO_2 into fuel products is being considered an appealing technology to reduce reliance on fossil fuels [21].

ERC is an interesting approach to convert CO_2 because of the following benefits: (1) Water serves as the proton source; (2) there is high equilibrium conversion at ambient temperature and pressure; and (3) the process is reasonably simple and environmentally friendly. These advantages are increasing attention and rapidly developing in the use of electro catalysts for CO_2 reduction to diverse carbon compounds [22].

Catalysts	**products**
Solid oxide fuel cells	
Platinum	CO
Nickel	CO, methane CO
Palladium	CO
Copper	CO
Metallic electrodes in aqueous solution	
Copper	Hydrocarbons, CO, formate, alcohols,
Platinum	CO, methanol

Others (Pb, Oxide-derived Au)	CO, formate
Molecular electrocatalysts	
Copper complexes	oxalate
Palladium complexes	CO, formic acid
Nickel complexes	CO, oxalate, formic acid, formaldehyde
Cobalt complexes	CO, formic acid, alcohols

Table 1 The electrochemical reduction products of CO_2 over various catalysts.

2.4. Mechanism of electrochemical reduction of CO_2

CO2 has the highest thermodynamic stability due to its strong C-O double bond, which has a bonding energy of 750 kJ mol-1. The bond strength of C-C is 336 kJ mol−1, C-O is 327 kJ mol−1, and C-H is 411 kJ mol−1. CO_2 reduction by electro catalytic method is a thermodynamically uphill reaction that requires a significant amount of energy to break the C=O bond. To make matters even more challenging, CO_2 reduction can occur by a variety of chemical routes, transferring 2, 4, 6, 8, 12, or even more electrons and creating a range of products such as carbon monoxide (CO), formic acid (HCOOH), methane (CH_4), ethylene (C_2H_4), and others. Its multistep electrochemical reduction is far more difficult than water splitting. Any chemical conversion of CO_2 to fuel requires a considerable amount of energy, proper reaction conditions, and active catalysts. Chemical reaction conversions, on the other hand, are driven by differences in Gibbs free energy between the reactants and products of a chemical reaction under specified conditions. The enthalpy term is a good starting point for assessing the thermodynamic stability and viability of any CO_2 conversion[23][24][25]. Electro catalytic carbon dioxide follows several chemical paths to yield distinct compounds.

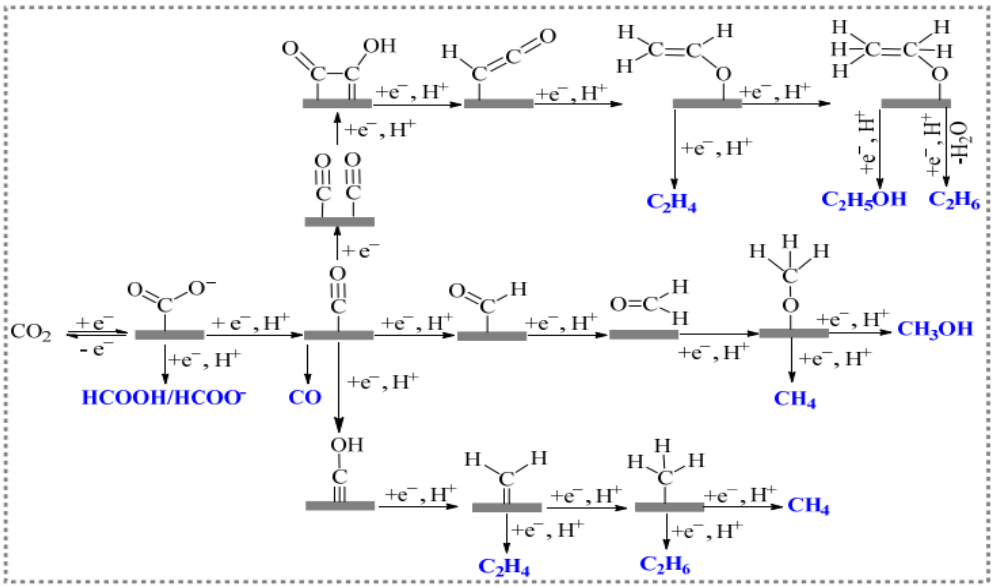

Figure 1 Possible reaction pathways for the electro-reduction of CO_2 [26].

2.5. Catalyst Engineering

Catalysts are critical components of catalytic reactions that influence reaction rate and selectivity. Studies have shown that catalytic modification of Cu-based catalysts can significantly enhance their inherent activity and selectivity toward the C_{2+} products of CO_2RR[27][28]. Catalyst engineering, for example, can control the electrical structure of catalysts, govern their tiny microstructures, produce a large number of active sites, and modulate the binding strength of critical intermediates. Consequently, the activity and selectivity of Cu-based catalysts toward high-value C_{2+} products can be adjusted [29]. Catalyst engineering for Cu-based catalysts that convert CO_2 to C_{2+} products, including composition, morphology, crystal phase, facet, defect, strain, surface and interface, and underlying mechanisms [16].

2.5.1. Composition

Composition management is a typical technique for influencing the catalytic performance of Cu-based catalysts by varying the element species, element ratio, and chemical state of Cu. Typically, composition control of Cu-based catalysts is classified into two categories based on the type of component [30]. One method is to mix Cu with other metal components to create Cu-based

bimetallic/multimetallic catalysts[31]. Another method is to add nonmetal elements to Cu to produce Cu-based compound catalysts. Recent studies have shown that composition management of Cu-based catalysts can accelerate the synthesis of C_{2+} products of CO_2RR, which is related to several effects such as synergistic impact, alloying effect, tandem effect, chemical state effect, and microstructure effect[32].

2.5.1.1. Metal Elements

When copper (Cu) is combined with other metals, the performance of copper-based catalysts in the carbon dioxide reduction reaction (CO_2RR) can be greatly enhanced. This improvement is attributed to the interplay of ligand effects, electronic effects, and geometric effects between the different metals [33][34][35]. So far, several metals known for their inherent CO_2RR catalytic activity, such as gold (Au), silver (Ag), palladium (Pd), gallium (Ga), tin (Sn), lead (Pb), bismuth (Bi), and zinc (Zn), have emerged as promising candidates. For instance, Jaramillo et al. explored the CO2RR performance of a series of CuAg thin films with adjustable compositions, spanning from copper-rich to silver-rich compositions [19]. The CuAg catalysts with different silver concentrations exhibited distinct product selectivities compared to those of pure copper and pure silver.

2.5.1.2. Non-Metal Elements

On top of using metal parts, throwing in some nonmetal ingredients like boron, nitrogen, oxygen, selenium, and halogens with the copper can boost how well copper-based catalysts work at turning CO_2 into valuable C_{2+} products. When copper gets together with these nonmetal ingredients, they make copper compounds. Copper compounds in high spin states are very effective in converting CO_2 into C_{2+} products such as ethylene (C_2H_4) and ethanol (C_2H_5OH) via electroreduction. For example, copper(I) compounds combined with boron, nitrogen, selenium, or halogens can boost ethylene production during CO_2 electroreduction [36][37][38][39].

2.5.2. Facet

The varying structures of metal nanomaterials can reveal facets with diverse orientations. This, in turn, influences the regular pattern of atomic arrangement, the strength of metal bonds, and the energies associated with adsorption and binding of intermediates. Consequently, these factors significantly impact the catalytic performance in ECR processes [40][41][42][43].

Copper's special talent for turning carbon dioxide into hydrocarbons and alcohols mainly comes from its ability to bind carbon monoxide in specific ways and stabilize key reaction. Because of this, we can fine-tune what products copper makes by changing which of its crystal surfaces are exposed. For example, the (111) surface of copper is great for making methane, while the (100) surface is better for making ethylene. On the other hand, the (110) surface encourages the production of ethanol, acetate, and acetaldehyde [44][45][46][47].

Research has shown that the different reaction pathways and intermediates on the (111) and (100) crystal facets play a crucial role in determining the ultimate selectivity of ECR [48]. On Cu (111) facets, *CO intermediates tend to form *CHO or *COH intermediates, which can then be further reduced to CH_3OH or CH_4, respectively [49][50][51] . Meanwhile, Cu(100) facets facilitate the dimerization of *CO, leading to the formation of either C2H4 or C_2H_5OH after subsequent proton and electron transfer [52][39][53][54]. So, it's really important to have a lot of *CO absorbed on the surface to selectively make ethylene. Just lately, De Gregorio and colleagues [55]. Made copper nanocrystals (Cu NCs) in different shapes. These were used to selectively turn CO_2 into ethylene and methane, with high efficiency and production rates, all in a gas-fed flow cell.

2.5.3. Definition and Classification of Defects

The term “defect” was first defined by Tate v. Latham and Son in 1897 as a lack or absence of something essential to completeness. In current scientific terminology, however, defects are distortions of periodic structure in full crystals. For crystalline materials, defects can be classified depending on their position into bulk defects and surface defects. Surface defects, including point defects, line defects, and plane defects, have been widely exploited in electrocatalysts to modulate electronic structure and surface/interface properties. Point defects, which exhibit deviation from the normal crystallographic arrangement in the nodes or adjacent regions, are quite effective and most commonly used in electrocatalytic process. Depending on their origin, point defects can be categorized as doped defects and intrinsic defects. Doped defects occur when a heteroatom/particle replaces a normal atom/particle or occupies a gap position in the normal node. An intrinsic defect is a vacancy in the lattice node or an extra particle (gap particle) in a gap that should be vacant. Generally, the classification of defects is becoming increasingly diversiform and complicated as knowledge of the field expands [56].

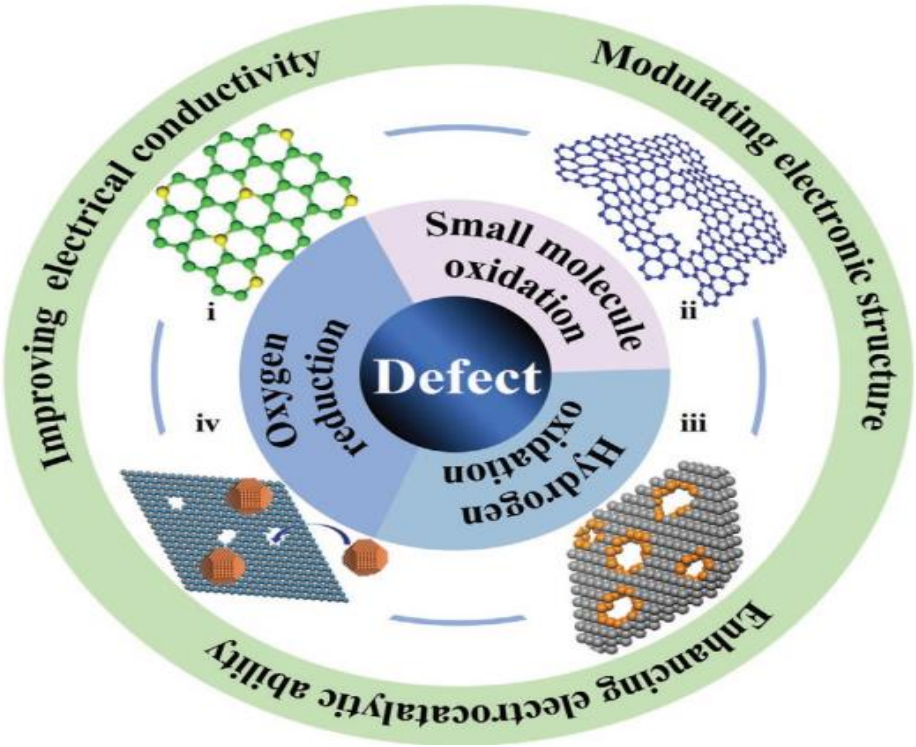

Figure 2 Some of the basic concepts in defective electro catalysts for ORR, HOR, and SMOR. i) Heteroatom doping, ii) intrinsic defects, iii) defective PGM catalysts, and iv) defective supports [56].

2.5.4. Morphology

The morphology of Cu catalysts, including their size and shape, significantly impacts their catalytic performance. Nanostructured Cu, such as nanoparticles or nanowires, can provide a higher surface area and more active sites for CO_2 reduction. Tailoring the morphology can also influence the distribution of active sites that favor the formation of C_{2+} products over CO or methane [9][57].

2.5.5. Crystal Phase

The crystal phase of Cu can affect its catalytic properties. Different phases, such as Cu(I) and Cu(II), exhibit distinct reactivity towards CO_2. Engineering the crystal phase through controlled synthesis methods can enhance the catalyst's performance by stabilizing specific active sites that are more favorable for C_{2+} product formation [58].

2.5.6. Strain

Strain engineering involves applying mechanical stress to the catalyst, which can alter its electronic structure and reactivity. Strained Cu surfaces may exhibit enhanced catalytic activity due to changes in bond lengths and angles, which can stabilize reaction intermediates and promote the desired reaction pathways [80].

2.5.7. Surface and Interface Engineering

The surface and interface characteristics of Cu-based catalysts are critical for their performance. Modifying the surface chemistry, such as by functionalizing with specific ligands or creating heterostructures with other materials, can enhance the interaction between the catalyst and CO_2. This can lead to improved selectivity and activity for C_{2+} products [59].

2.6. Structural Properties of Crystal Covellite (CuS)

Covellite (CuS) is a bulk material that's part of the layered chalcogenide family. Its crystal structure falls under the P63/mmc (No. 194) space group, forming a hexagonal unit cell at room temperature. This unit cell contains 12 atoms, with lattice parameters a=3.796 and c=16.382, leading to a calculated density of 4.66g/cm³ [60]. Covellite has a layered structure made up of alternating CuS3 units (arranged in triangular planes) and CuS4 units (arranged in tetrahedra), connected by S-S bonds, which are significant in the chemistry of sulfides. Covellite (CuS) is a naturally occurring green-black copper sulfide mineral that mainly forms after supergene enrichment processes in copper ore deposits. However, it can also be artificially synthesized through methods like solution growth or solid-state vapor reactions [61][62][63].

Covellite is a mineral with distinct layers of metal, held together by fairly strong bonds between the sulfur atoms. Imagine its structure like thin plates linked by these S-S bonds. On its own, it's not very stable, but with the right support, it can achieve stability and resembles a graphene-like arrangement. Because of its interesting light and electronic properties, CuS has garnered significant interest, especially for use as a catalyst [64][65][66].

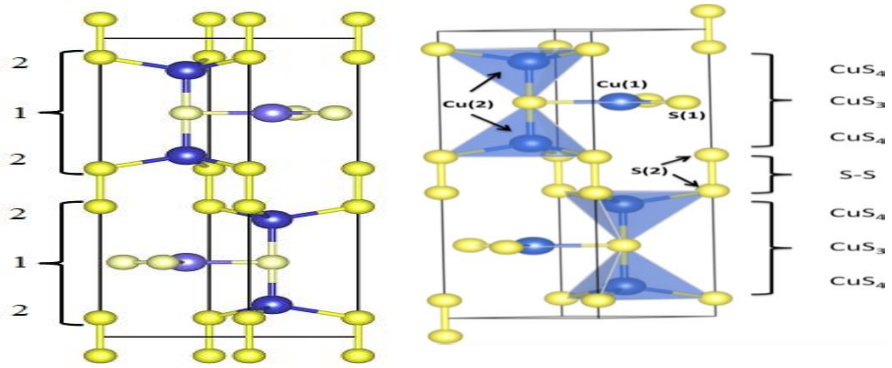

Figure 3 Illustrates the structural features of a covellite (CuS) hexagonal unit cell, highlighting the connections between copper (Cu) and sulfur (S) atoms, as well as sulfur-sulfur (S-S) bonds.

The copper atoms are shown in two different geometrical arrangements: tetrahedral (labeled as 2) and trigonal planar (labeled as 1). The visualization is presented in two styles: a) ball-and-stick model, and b) polyhedral representation. In both models, blue spheres represent copper atoms, while yellow spheres represent sulfur atoms [65][66]

In Figure 3, the sulfur atoms are arranged trigonally around the copper atom labeled Cu(1), while those surrounding Cu(2) form a tetrahedral shape. These two configurations are frequently observed in sulfide compounds. Because of their unique electronic, structural, and bonding characteristics, the trigonal planar and tetrahedral arrangements of copper atoms associated with the two distinct sulfur atom binding sites in covellite have been extensively studied. Notably, the copper atom within CuS exhibits lower toxicity compared to atoms like lead, cadmium, and arsenic found in other semiconductor materials.

lattice parameter, bond angle	**Exp.**	**GGA**
a=b (Å)	3.7938,3.76	3.826
C (Å)	16.341	16.596
Cu(1)-S(1) (Å) x3	2.190s	2.208
Cu(2)-S(1) (Å)	2.331	2.374
Cu(2)-S(2) (Å) x3	2.305	2.322
S(2)-S(2) (Å)	2.071	2.113
S(1)-Cu(2) -S(2)	108.16	
V_0 (Å^3)	202.5,199.9	208.13

Table 2 compares calculated and experimental data for CuS, covering lattice parameters, bond lengths, bond angles, and cell volume [67] [68].Let's take a look at how well our calculations on chemical bonding and structural properties match up with real-world experimental data, as shown in Table 2. When we use the GGA level of theory for analysis, we find that the lengths of the Cu(2)-S(1) and S(2)-S(2) bonds are slightly overestimated. Specifically, they're off by less than 0.043 Å and 0.042 Å, respectively, when compared to the actual experimental values.

2.7. Use of copper sulfide for electrochemical reduction of carbon dioxide

Copper sulfide compounds have a long history as catalysts in electrochemical reactions, especially in reducing CO_2. The way sulfur atoms bond can differ greatly. For instance, sulfur, with its low electronegativity, readily forms ionic compounds with metals and can also bond with itself to create chain-like polysulfide ions like Sn_{2-}. Due to sulfur's diverse bonding capabilities, sulfide structures are both varied and complex, making sulfur an attractive option for modifying electrocatalysts. Copper sulfide compounds, depending on the sulfur content, how it's combined, and the other elements present, display a range of phases, shapes, and crystal structures. They're used extensively in fields like catalysis, optoelectronics, solar cells, sensors, biomedicine, and more. In the context of electrocatalytic CO_2 reduction reactions (CO_2RR), sulfur atoms can effectively dampen the hydrogen evolution reaction (HER) and also alter how strongly CO_2 reduction intermediates are absorbed and released. For that reason, copper sulfide compounds have promising prospects for improving catalytic activity and product selectivity [9].

CHAPTER THREE

3. Computational Methodology

We use a software package called QUANTUM ESPRESSO to run electronic structure calculations with a method called DFT. For the electronic exchange-correlation energy, we use approximations known as Perdew-Burke-Ernzerhof and generalized-gradient. Our simulations start with the basic repeating unit of a crystal, and the data for this unit is saved in a file format called cif. This cif format is designed to be easily understood by both people and computers for describing crystal structures. To make this data usable for our simulations, we employ a tool called Cif2cell to transform the crystal data from cif format into the specific input format needed by QUANTUM ESPRESSO. This software, QUANTUM ESPRESSO, has its own way of reading crystal structure data, so we convert the cif file into a format it can understand. The last step is to create the input file that we'll use in our calculations down the line. It's worth noting that QUANTUM ESPRESSO is open-source software, meaning its use is governed by the GNU General Public License, and it includes not just DFT methods but also associated codes. Quantum ESPRESSO (QE) uses the PWscf module to handle self-consistent calculations, a crucial step for the rest of the system to work correctly. We ran these calculations on a 64-bit Linux operating system. All our calculations for bulk CUS were done using Quantum ESPRESSO. This involved looking at convergence for various parameters such as the K-mesh, lattice constant, Ecutwfc, Ecutrho, and the band structure.

3.1. Density Functional Theory (DFT)

Density Functional Theory, or DFT, is a widely used computational method in fields like condensed matter physics, chemistry, and even biology. It's used to investigate the electronic structure of systems with many electrons, and it does this by focusing on electron density. The name "density functional theory" comes from the fact that it analyzes many-body systems through electron density functions instead of wave functions. A key advantage is that by using electron density instead of wave functions, the complex, multi-dimensional problem of many-electron

systems simplifies to a more manageable three-dimensional one, significantly easing the computational workload.

3.2. Pseudopotentials

Compared to those lively valence electrons, an atom's core electrons often play a smaller role. Because core electrons have really fast, short-range oscillations, they often force us to use super high energy cutoffs in plane wave calculations when we're modeling how atoms interact. To get around this bottleneck, we can use what's called pseudopotentials to approximate an atom's core electrons in a system. These essentially assign a kind of "effective density" to the electrons within a certain radius, beyond which we don't worry about them. This trick lets us use a much lower energy cutoff, and it also shrinks our system by letting us focus only on the valence electrons. Density Functional Theory (DFT) methods can employ various types of pseudopotentials, with the three most popular being ultrasoft pseudopotentials (US-PP)[69], the projected augmented wave (PAW) method, and norm-conserving pseudopotentials (NC-PP) [70].

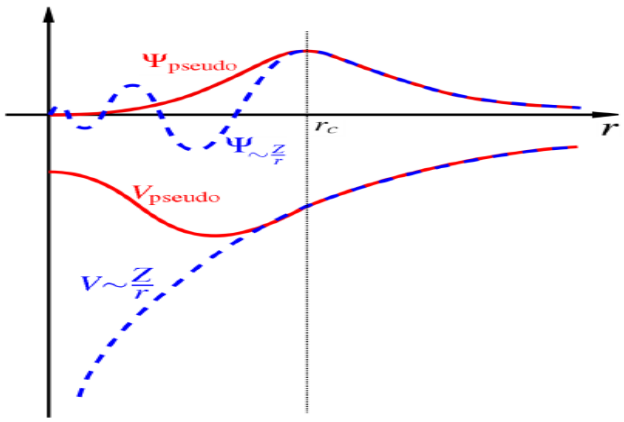

Figure 4 How the coulomb potential wavefunction stacks up against the pseudopotential wavefunction.

The red curves show us the behavior of the pseudopotential, while the blue ones represent the coulomb potential. Interestingly, once we pass a certain point called the cut off radius (rc), both types of wavefunctions align perfectly with each other [92].

3.3. Software Package

3.3.1. Quantum ESPRESSO Software Package

The computations outlined in this thesis were carried out using the open-source software known as Quantum-ESPRESSO (QE). QE offers a comprehensive collection of computer codes specifically designed for electronic structure calculations and materials modeling. These codes utilize density functional theory (DFT), a plane-wave basis set, and pseudopotentials to accurately depict the interactions between electrons and ions [71]. ESPRESSO is a free, open-source software bundle designed for research in electronic structure, simulation, and optimization. It's distributed under the GNU General Public License, often referred to as the GPL [72]. Quantum Espresso (QE) uses a clever method to do its calculations. It solves the Kohn-Sham equations repeatedly, fine-tuning the results each time, and also uses efficient ways to mix the charge density. This allows it to figure out the forces acting on atoms and the stresses within a unit cell. The total energy is adjusted until it's as low as possible, based on where the atoms are located inside the unit cell.
This software package comes with a program called PWscf, which is used for calculating total energy. PWscf uses both Norm-Conserving Pseudopotentials (NC-PP) and Ultrasoft Pseudopotentials (US-PP) within Density Functional Theory (DFT). When doing DFT calculations, it's important to pay attention to two things to make sure your results are accurate. First, you have to consider the energy cutoffs, which basically set a limit on how much the wave functions can be expanded. Second, you need to think about the number of k-points. This tells you how well your discrete grid represents the continuous integral [73].

3.3.2. Visualization for Electronic and Structural Analysis –VESTA

VESTA, which stands for Visualization for Electronic and Structural Analysis, is a powerful tool used for visualizing both three-dimensional crystal structures and volumetric data, all within a user-friendly interface that features multiple windows and tabs. When it comes to representing crystal structures, VESTA offers a variety of models including ball-and-stick, space-filling, polyhedral, wireframe, dot-surface, and thermal-ellipsoid. The software also allows users to extract

a wealth of crystal-chemical information from site data, such as fractional coordinates, occupancies, and oxidation states. With its support for multiple windows, each containing multiple tabs for different graphics pages, users can easily switch between different visualizations with a simple click of the mouse. All the information needed to recreate the visual representation of each page is stored in a compact text file, called a "*.vesta" file, using the VESTA format. This method is incredibly adaptable, allowing us to handle massive quantities of objects like atoms, bonds, coordination polyhedra, and polygons on isosurfaces, provided there's sufficient memory available. These objects can be swiftly rotated, resized, and moved around in three dimensions[74]. The software package used to build and visualize the copper sulfide surface plane in this study is called VESTA.

3.3.3.MATERIALS STUDIO

Materials Studio (MS) was used for constructing molecular models, conducting classical simulations, and executing quantum mechanical calculations. The MS package offers a variety of modeling methods, which is evident from the wide range of articles published. The user interface, designed for the Windows operating system (unlike, say, UNIX or Linux), made the software accessible to a larger audience (especially back then), particularly within the research and development divisions of major chemical firms [75].This software allows us to figure out the lattice parameters and electronic structure of a material by employing quantum mechanical methods. We'll use this software to study how CO_2 molecules adsorb onto the surface of a CuS plane. The CuS surface in question was generated from an optimized bulk CuS structure, a process carried out using Material Studio.

3.3.4. XCrySDen

XCrySDen is a software tool used to visualize crystalline and molecular structures. Its name, an acronym for Crystalline Structures and Densities, includes an "X" because it operates within the X Window system. This program allows users to view isosurfaces and contours, which can be overlaid on crystal structures and freely rotated or altered. Furthermore, it offers analytical tools for studying properties in reciprocal space, including interactively choosing k-paths within the

Brillouin zone for band-structure diagrams and visualizing Fermi surfaces. As an additional feature, XCrySDen provides a graphical user interface for visualizing data from Quantum ESPRESSO. XCrySDen is a program designed for visualizing molecular and crystalline structures, though its primary function is for analyzing properties. It operates on most UNIX systems, requiring no specific hardware or software. Significant attention has been dedicated to enabling the appropriate display of 3D isosurfaces and 2D contours, which can be overlaid on the crystalline structure and interactively rotated and manipulated [76].

3.4.The PWscf method

The Kohn-Sham equations are pretty tricky to solve because they're highly nonlinear. That means we have to tackle them using an iterative method. PWscf does just that - it iteratively solves these equations until it reaches a self-consistent solution. This involves repeatedly diagonalizing matrices at each step within the framework of the plane wave pseudopotential approach. Here's how the self-consistent calculation works: it starts with an initial guess for the electron wave functions. Using these, it calculates the corresponding effective Kohn-Sham potential, which we call VKS. Then, it solves the Kohn-Sham equation again using this new potential, which gives us updated wave functions. This back-and-forth process continues until the charge density stops changing significantly. At this point, we've achieved self-consistency, meaning the wave functions and the effective potential are in agreement. In essence, the wave functions we obtain are the same as those we'd get by solving the Schrödinger equation with that particular potential. The PWscf method includes both norm-conserving and ultrasoft pseudopotentials.

3.4.1. Input File for a Simple PWscf Calculation

The PWscf input file consists of several NAMELISTS and INPUT_CARDS. NAMELISTS enable you to specify the value of an input variable only when necessary, while automatically assigning default values to most variables that don't require explicit specification. They are read in a predetermined order but can be disregarded if they're not relevant. In PWscf, you must include three NAMELISTS. The first is &CONTROL, which includes the input variable that governs the calculation's flow and determines the amount of input/output displayed on the disk and screen. The

&SYSTEM namelist defines the characteristics of the system being studied. The third required NAMELIST is &ELECTRONS, which encompasses the input variables that manage the algorithms used to achieve a self-consistent solution of the Kohn-Sham equations for the electrons.

On the flip side, INPUT_CARDS come into play when you need to supply essential data that would be a real drag to input repeatedly using the `variable_name = variable_value` format found in NAMELISTS. There are three INPUT_CARDS that are absolutely essential. The ATOMIC_SPECIES card is where you list the name, mass, and pseudopotential for every type of atom in your system. Then, you've got ATOMIC_POSITIONS, which details the type and exact location of each atom within the unit cell. Finally, K_POINTS is the last required INPUT_CARD, and it handles the integration of the Brillouin zone.

3.5. Adsorption Energy

Adsorption is all about molecules sticking to a surface, and a key part of this is how much energy is involved in the process, which we call adsorption energy. This energy is a big deal because it tells us how stable the adsorption is.

Think of adsorption energy as the energy difference between what you start with (reactants) and what you end up with (products). If the energy is negative, it means the products are more stable, and the molecule wants to stick to the surface – it's like a natural fit. This is also an exothermic process, meaning it releases heat. The more negative the energy, and the higher the adsorption, the more favored (and stable) the structure or adsorption site is. On the flip side, a positive energy suggests that the molecule doesn't really want to stick to the surface [77].

$$E_{ads} = E_{Surface+Species} - E_{Surface} - E_{Species} \quad \text{.....} \quad 22$$

Where the term "E Surface+species" refers to the overall calculated electronic energy of the surface combined with the particular species within the system when it's in equilibrium. "ESurface" is the total electronic energy of just the slab (meaning a clean surface), and "ESpecies" stands for the total electronic energy of the species alone (as if it were a free molecule).

CHAPTER FOUR

4.Results and Discussions

4.1. Convergence tests of bulk CuS

To optimize the geometry, you'll want to run the "relax" calculation in your input file. The bulk CuS we're dealing with has a hexagonal structure, specifically with `ibrav = 4`. Before diving into the full calculations, it's crucial to do a convergence test; this ensures our results are numerically reliable. We absolutely need to choose an exchange-correlation functional, and for this entire study, we're using the PBE exchange-correlation functional. The pseudo-potential files for the bulk CuS were sourced from the cifcell database. These files also gave us the recommended minimum cutoffs for both wave functions and charge density. When it comes to choosing the K-mesh for the geometry optimization, we tested a range of grids, starting from 1x1x1 all the way up to 11x11x11. We performed various convergence tests, looking at the K-mesh, the kinetic energy cutoff for wave functions, and the cutoff for charge density. Ultimately, we found a set of criteria that gave us converged results, meaning we reached the minimum total energy.

This chapter is all about diving into the best structure for bulk copper sulfide, looking at how well our analysis converges, and finding the ideal setup for a pure CuS (110) surface. We also explore what happens when we add zinc to CuS, create a copper defect in CuS, and figure out the energy it takes for things to stick to these materials.

4.2. optimization of bulk CuS

4.2.1. Analysis of Kinetic energy cutoff, charge density cutoff and K-points grid

To figure out the best settings for our calculations on CuS materials, we ran some convergence tests. These tests helped us find the ideal cutoff energy, charge density cutoff, and K-points. We wanted to see how these parameters affected the total energy calculations and find the lowest energy possible. The results of these tests are shown in Figure 11. We also performed tests to find

the right kinetic energy cutoff (ecutwfc) and charge density cutoff. These are important because they affect how accurately we can describe the system using a plane wave basis and self-consistent field (scf) calculations for the total electronic energies. Getting these values right helps us get a true picture of what the CuS material is like. The kinetic energy and charge density cutoffs are theoretical parameters that control the accuracy of our description and are related to the pseudopotential used for the initial optimized structure. To perform this calculation, which involves various convergence tests, we used a plane wave basis set with a cut-off energy of 60 Ry for the Kohn-Sham wave functions. The charge density cut-off was set to 450 Ry, and a k-point grid of 4x4x4 was employed. For the variable unit cell relaxation (vc_relax) calculations aimed at optimizing the geometry of the bulk structure, the convergence threshold for the self-consistent field energy was set to 10^-8 Ry. We utilized the PBE exchange-correlation functional, ultrasoft pseudopotentials, and the Monkhorst-Pack method for Brillouin zone sampling [78], using a 4x4x4 k-point grid for the bulk and a 3x3x1 grid for the slab to account for the vacuum introduced. This chosen set of parameters was consistently used across all calculations for both the bulk and slab (surface) models. The specific choice of k-points was made because it represents the minimal convergence point on the curve, ensuring a good balance between computational efficiency and the accuracy of the results. We visualized the structures using the XCrySDen and VESTA software packages.

4.2.1.1. Convergence test for k-point grids

To test the convergence of K-points, we ran SCF calculations with K-points ranging from 1x1x1 to 11x11x11. We then plotted the total energy against the K-points, and the results are presented in Figure 7.

Figure 7 indicates a convergence test for k-point grids, commonly used in computational materials science and quantum chemistry to sample the Brillouin zone for electronic structure calculations. The x-axis represents the "K point," while the y-axis displays energy values in Rydbergs (Ry), allowing for an examination of how energy varies with different k-point densities. Various configurations, such as "111000," "222000," and "333000," indicate different sampling schemes, with the plotted data showing a rapid convergence toward a stable energy value as k-point density increases. The sharp initial drop in energy suggests that adequate k-point sampling is critical for accurate calculations. The "444000" emphasizes its significance as a point where the energy stabilizes, indicating that further increases in k-point density yield diminishing returns.

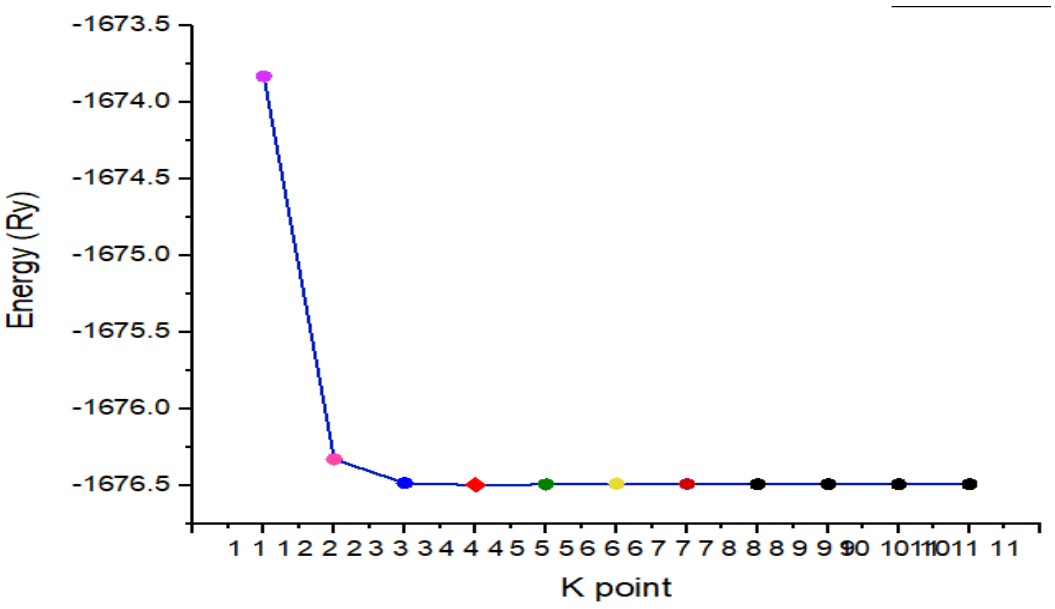

Figure 5 Convergence test for optimized bulk CuS. Total energy vs K points by using PBE

4.2.1.2. Convergence test for cutoff of wave function (ecutwfc)

We checked the convergence of the kinetic energy cutoff by adjusting the cutoff energy. The resulting plot of total energy versus kinetic energy cutoff can be seen in Figure 8. Figure 8 describes the relationship between "Ecutwfc," referring to a cutoff energy for wave functions in quantum mechanics, and corresponding energy values. The x-axis represents "Ecutwfc," while the y-axis shows energy levels, with specific points labeled as "ec20," "ec40," "ec60," and so on. The plotted points indicate how energy varies with different cutoff values, with "ec60" suggesting its significance as a critical or optimal value within the dataset. The line connecting the points reveals trends in energy sensitivity to changes in "Ecutwfc," and the"ec60" indicate a minimum energy configuration or an important feature.

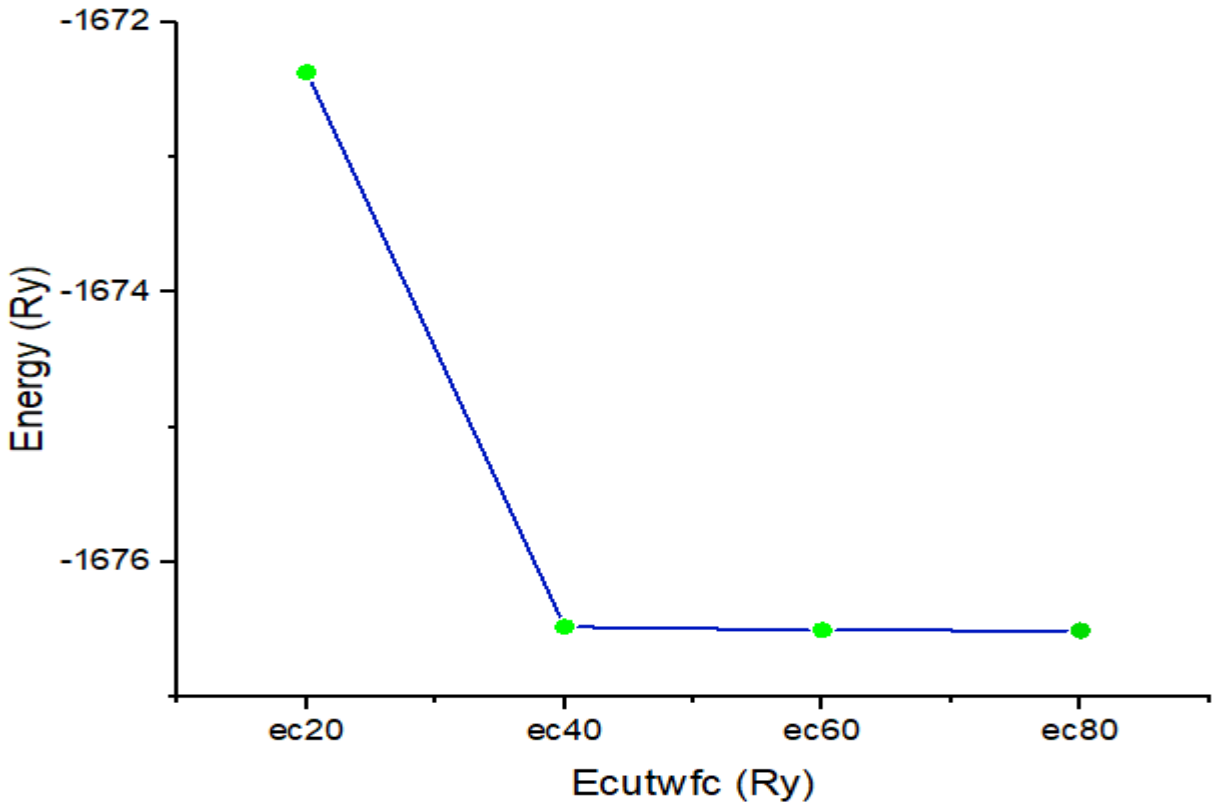

Figure 6 Convergence test for optimized bulk CuS. Total energy vs Kinetic energy cutoff by using PBE

4.2.1.3. Convergence test for cutoff charge density

To figure out the right charge density, we tried out different factors, ranging from 2 all the way to 10. Once we had that narrowed down, we used a kinetic energy cutoff value that settled at 60 Ry. We then took this 60 Ry value and multiplied it by each of those different factors to get a range of charge densities. Mathematically, that looks like this: Ecutrho = factor * 60 Ry. Finally, we charted the total energy against these varying charge densities (Ecutrho), and you can see the results in Figure 9.

Figure 9 presents a convergence test for cutoff charge density, a crucial aspect in computational materials science and quantum chemistry. The x-axis indicates "Ecutrho," representing the cutoff for charge density, while the y-axis displays energy values in Rydbergs (Ry). Various cutoff values, ranging from "100" to "600," are plotted against their corresponding energy values, revealing minor fluctuations that suggest energy stabilizes as the cutoff density increases. Notably, the point "450," with an energy value of approximately -1676.50776, emphasizes its significance as a critical point where energy reaches stability, indicating that further increases in charge density yield minimal changes in energy.

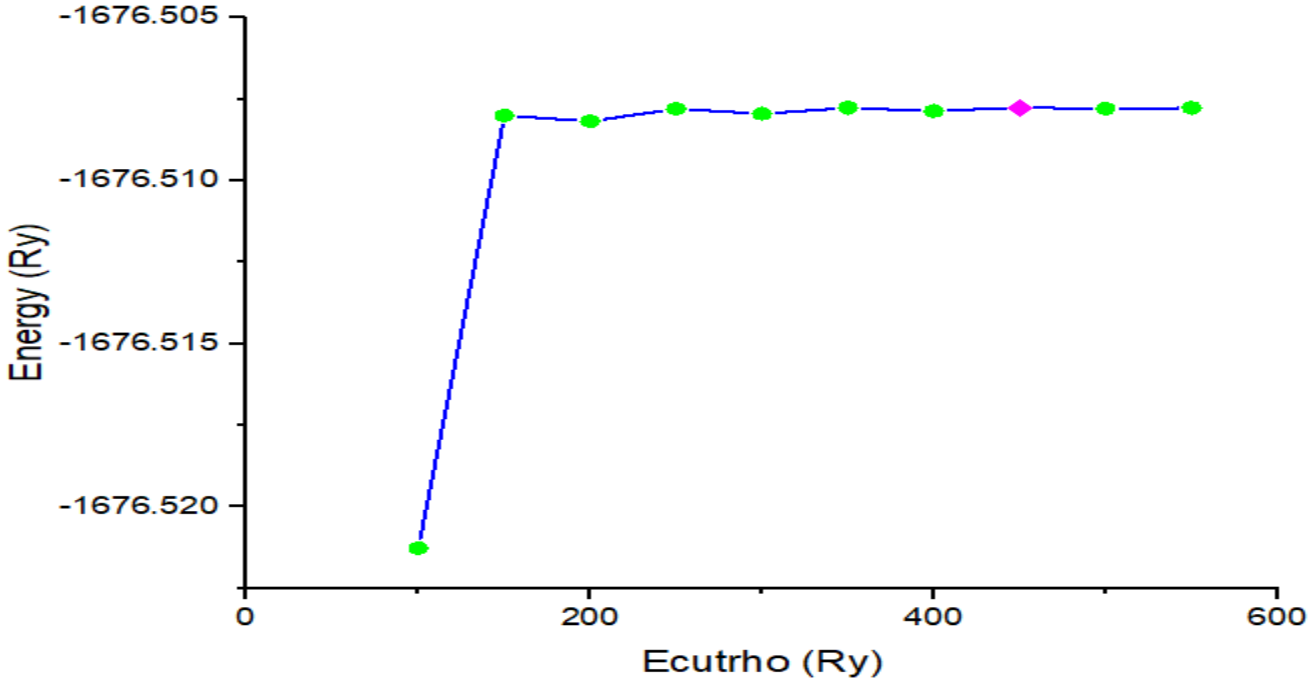

Figure 7 Convergence test for optimized bulk CuS. Total energy vs charge density cut-off energy by using PBE

4.2.1.4. Geometry optimization

To ensure our calculations for the lattice parameter were accurate, we used a convergence test. We set our parameters to commonly accepted values: a K-point grid of 4x4x4, a kinetic energy cutoff of 60 Ry, and a charge density cutoff of 450 Ry. Then, we tested a range of lattice constants, going up from 3.76786663 angstroms to 3.91786663 angstroms in one direction, and down from 3.76786663 angstroms to 3.67786663 angstroms in the other, with each step being 0.01 angstroms apart. We plotted the total energy against these lattice constants, and the results are displayed in Figure 10.

Figure 10 illustrates a graph pertaining to geometry optimization in computational materials science, where the x-axis likely represents atomic positions or a geometric parameter, and the y-axis displays energy values in Rydbergs (Ry). Various geometric configurations are plotted, showcasing fluctuations in energy as the optimization process explores different arrangements. Generally, the energy decreases as the geometric parameter progresses, indicating that the system is moving toward a more stable configuration. the point "3.80786663," with an energy value of approximately -1676.510677, marks it as a significant point where the energy is minimum, suggesting a successful optimization.

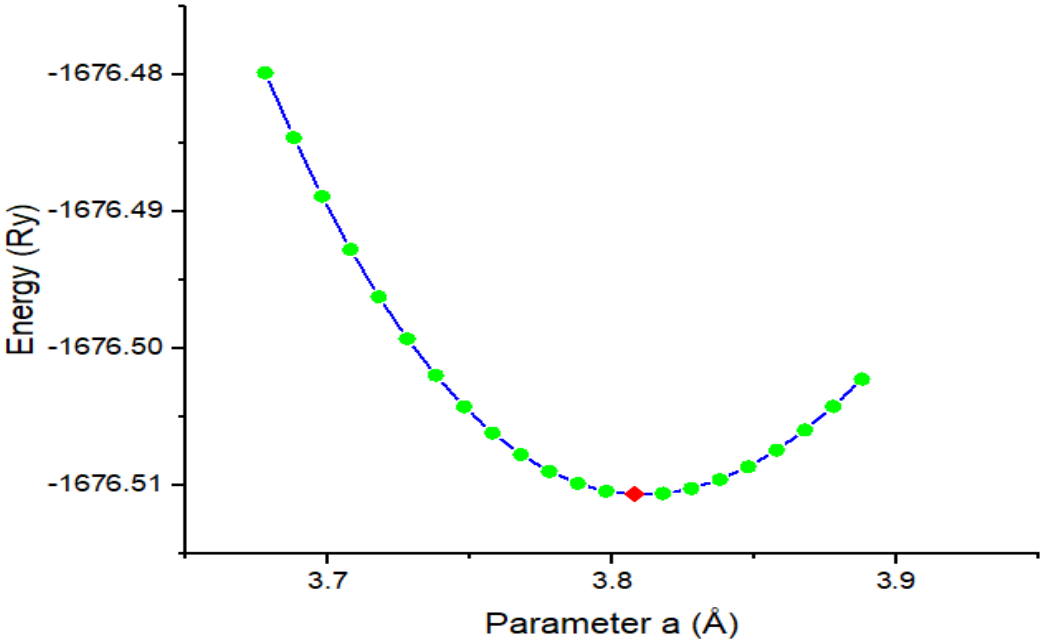

Figure 8 Convergence test for optimized bulk CuS.total energy vs parameter (a) by using PBE

Bulk CuS has a hexagonal unit cell structure. By starting with the initial crystal structure parameters of \(a = 3.80786663 \) Å and \(c = 16.48526376 \) Å, full geometry optimization calculations were carried out. These calculations characterized the cell parameters and the interatomic bond distances and angles, showing good agreement with experimental values (a = 3.8073 Å and c = 16.523 Å) [61]. We use this more laid-back framework to build models of CuS (110) surfaces.

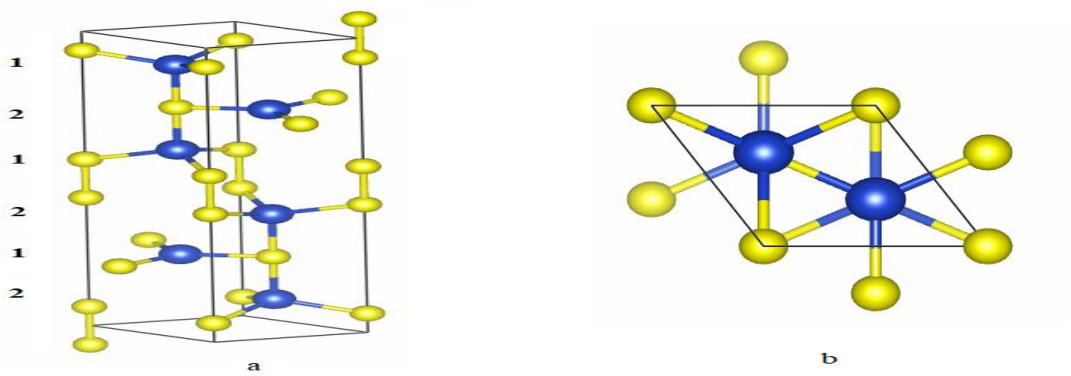

Figure 9. Optimized Covellite hexagonal unit cell (CuS).

(a) side view (b) top view . 1 and 2 represent Cu in tetrahedral and triangular position. Blue and yellow spheres are copper and sulfur atoms, respectively

Covellite	**Space group**	**Lattice parameter (Á)**	**Experimental**	**This work**
CuS	(P63/mmc)[79]	a=b c V c/a	3.796[79], 3.7938[66], 3.8073[61] 16.382[79],16.341[66],16.523[61] 204.4[79] ,202.5[66] 4.316[79],	a=3.80786663 Å , c=16.48526376 Å v=239.033781 Å^3 c/a=4.329265

Table 3: DFT optimized bulk CuS crystal structure parameters and comparison with experimental parameters

The calculated results presented in Table 3, including the lattice parameters a, b, c, and volume (v), show a strong agreement between our work and previous studies [80] [62] [74]. This structure is crucial for calculating the surface structure. In the surface calculations, we have taken into account parameters of bulk CuS, such as the cutoff energy and charge density cutoff.

4.3. Band structure Calculations

4.3.1. Band structure Calculations Copper sulfide

The band structure of copper sulfide (CuS) is a critical aspect of its electronic properties, significantly influencing its behavior as a semiconductor and its catalytic performance in reactions such as the electrochemical reduction of carbon dioxide (CO_2). CuS typically exhibits a narrow band gap, which can vary depending on its structural form (e.g., chalcopyrite, covellite) and the presence of defects or dopants. The valence band is primarily composed of sulfur (S) 3p orbitals, while the conduction band is largely derived from copper (Cu) 3d orbitals, leading to unique electronic properties that affect charge carrier mobility. Doping CuS with elements such as zinc (Zn) can modify its band structure by introducing new energy levels within the band gap, enhancing conductivity and catalytic activity by facilitating charge transfer processes. Additionally, defect engineering, through the introduction of vacancies or other defects, can significantly alter the band structure by creating localized states that influence recombination rates and overall catalytic efficiency. The band structure can also vary with different crystal facets of CuS, as facet engineering can lead to variations in surface electronic states, impacting the adsorption of reactants and activation energy for catalytic reactions. Computational methods such as density functional theory (DFT) are often employed to analyze the band structure of CuS, providing insights into its electronic properties and predicting how modifications will influence its performance in applications like CO_2 reduction. Overall, understanding and manipulating the band structure of CuS is essential for optimizing its use in sustainable energy applications. The band structure is a good way to visualize the wave vector-dependence of the energy states, the band-gap, and the possible electronic transitions.

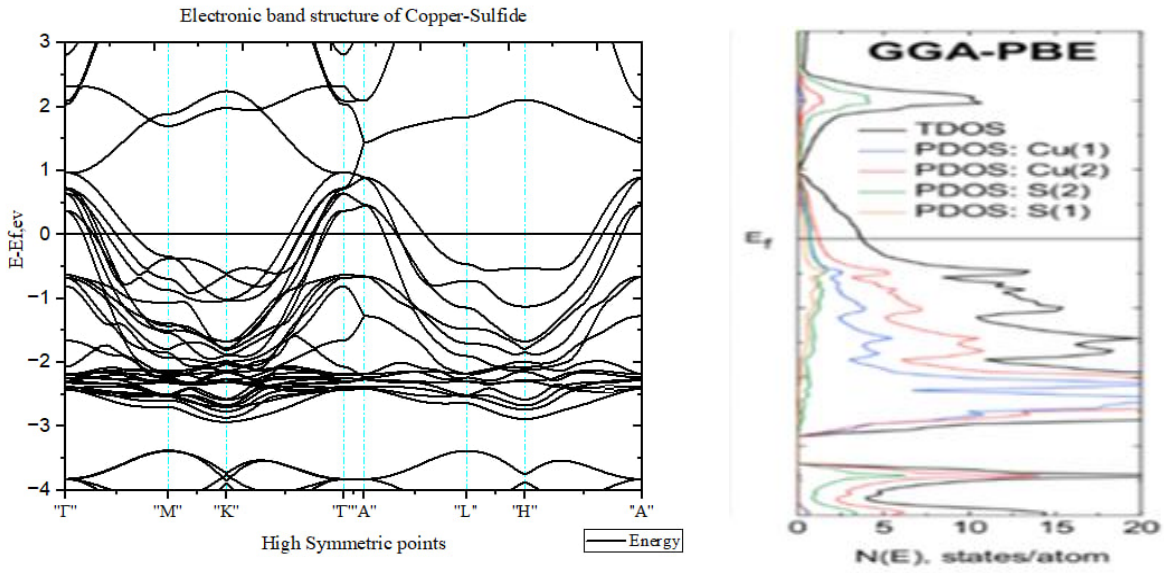

Figure 10 Band structure and density of state of CuS. GGA calculations The points Γ, M, and K are in the central plane (kz = 0) and A, L, and H are in the basal plane

Figure 12 shows the electronic band structure of CuS, showing the relationship between energy (E) and wave vector (k) across various high symmetry points in the Brillouin zone. The x-axis represents the wave vector, with high symmetry points such as Γ, M, K, L, and A indicating specific directions in the crystal lattice. The y-axis shows energy levels (E) relative to the Fermi energy (E_F), typically set at zero for reference. In this band structure, the bands can be categorized into valence bands and conduction bands. The presence of a gap between the highest filled band and the lowest empty band suggests that the material may exhibit semiconductor or insulator behavior, depending on the size of this band gap. A larger gap generally indicates insulating properties, while a smaller gap may suggest semiconducting characteristics and if there is no gap may suggest metallic characteristic. But this band structure shows there is no band gap have seen between valence bands and conduction bands so this material shows a metallic characteristic. The complexity of the band structure, illustrated by the multiple bands, indicates intricate electronic interactions within the material. These interactions can significantly affect its electrical, optical, and thermal properties. Analyzing the band structure is essential for understanding the material's behavior under various conditions, such as temperature and doping levels.

4.3.2. Band structure Calculations of Zn doped Copper sulfide

Band structure calculations of Zinc (Zn)-doped Copper Sulfide (CuS) are crucial for understanding the electronic properties and potential catalytic performance of this semiconductor material. When Zn is introduced into the CuS lattice, it typically substitutes for Cu, affecting the charge carrier dynamics by either acting as a donor or an acceptor. This doping can alter the positioning of the conduction and valence bands, consequently modifying the band gap, which is vital for optimizing catalytic properties. CuS usually possesses a narrow band gap, making it suitable for photocatalytic applications; therefore, assessing how Zn doping influences this gap through band structure analysis is essential. Furthermore, the introduction of vacancy defects in conjunction with Zn doping can lead to localized states within the band gap, which can trap charge carriers, improve charge separation, and enhance catalytic activity. Band structure calculations help elucidate the nature of these defect states and their influence on the electronic density of states. Additionally, facet engineering can expose different crystallographic facets, each with unique electronic characteristics, and understanding their band structures is critical for optimizing catalytic performance. Computational methods such as density functional theory (DFT), often utilizing tools like VASP or Quantum ESPRESSO, are employed to provide insights into these electronic modifications. Ultimately, these calculations offer valuable information on the electronic properties of Zn-doped CuS, linking them to enhanced catalytic activity for applications such as CO2 reduction and other energy conversion technologies.

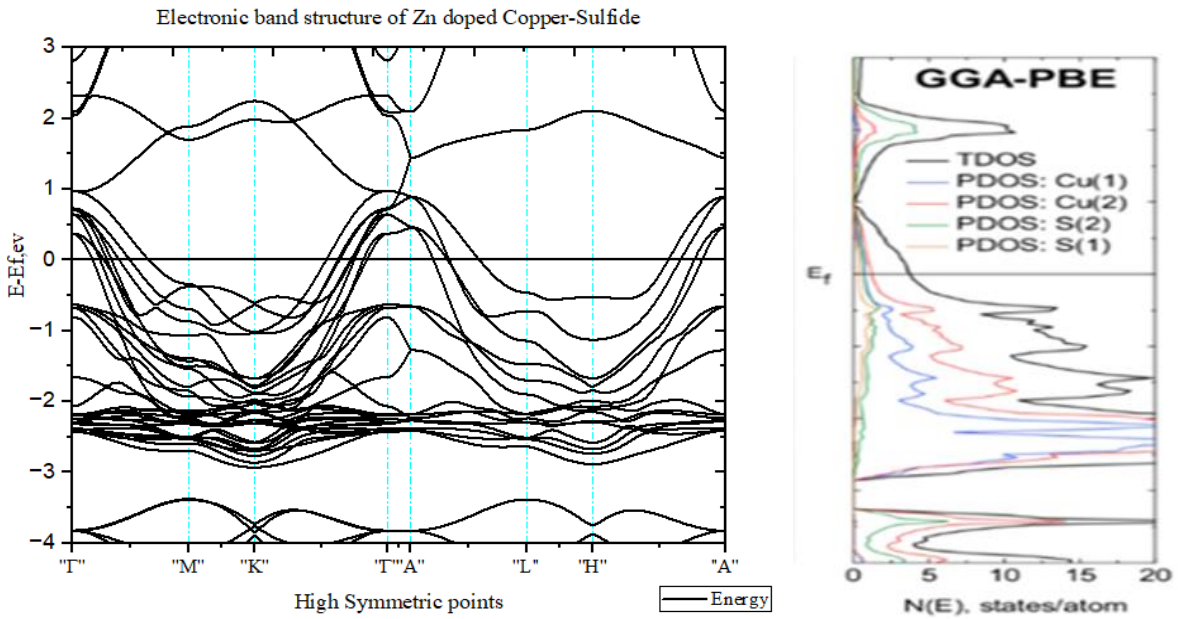

Figure 11 Band structure and density of state of Zn doped CuS. GGA calculations The points Γ, M, and K are in the central plane (kz = 0) and A, L, and H are in the basal plane

Figure 11 illustrates the electronic band structure of zinc-doped copper sulfide (Zn-doped CuS), presenting energy (E) on the vertical axis and momentum (k) along high-symmetry points in the Brillouin zone on the horizontal axis. The lines in the graph represent the allowed energy levels for electrons, with the labeled points (T, M, K, A, L, H) corresponding to specific locations in the Brillouin zone. The separation of the bands into occupied (valence) and unoccupied (conduction) states indicates the material's electronic behavior, helping to determine whether it acts as a conductor, semiconductor, or insulator. The energy difference between the top of the valence band and the bottom of the conduction band reveals the band gap, which can be direct or indirect. Doping with Zn can significantly alter the electronic properties of CuS by introducing new energy levels or modifying existing ones, thereby impacting conductivity and other characteristics. Understanding this band structure is essential for applications in electronics and optoelectronics, especially in developing materials for devices such as solar cells and LEDs.

4.4. Calculation Optimized of Pristine CuS (110) Surface

To figure out the ideal structure of a surface, we start with some key details from the material's bulk form. We need the lattice parameter, an energy cutoff set at 60 Ry, a charge density cutoff energy of 450 Ry, and the atomic coordinates. Then, we use software like Material Studio and VESTA to essentially slice the surface off the optimized bulk along the (110) plane. The resulting slab of CuS (110) has 4 layers of atoms and a total of 60 atoms (30 copper and 30 sulfur). To make sure there's no interference, we leave a 15 Å gap of empty space perpendicular to the surface.

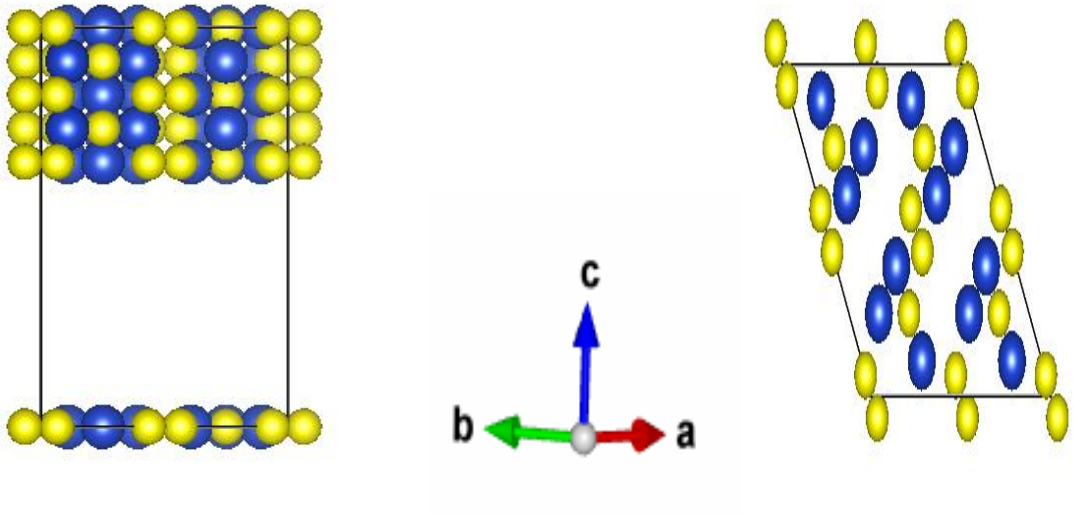

a b

Figure 12 The computational models of pristine CuS (110) surface optimized structure. (a)along a axis and (b) along c axis

4.5. Optimized of Pristine CuS (110) Surface adsorbed carbon dioxide with several active site

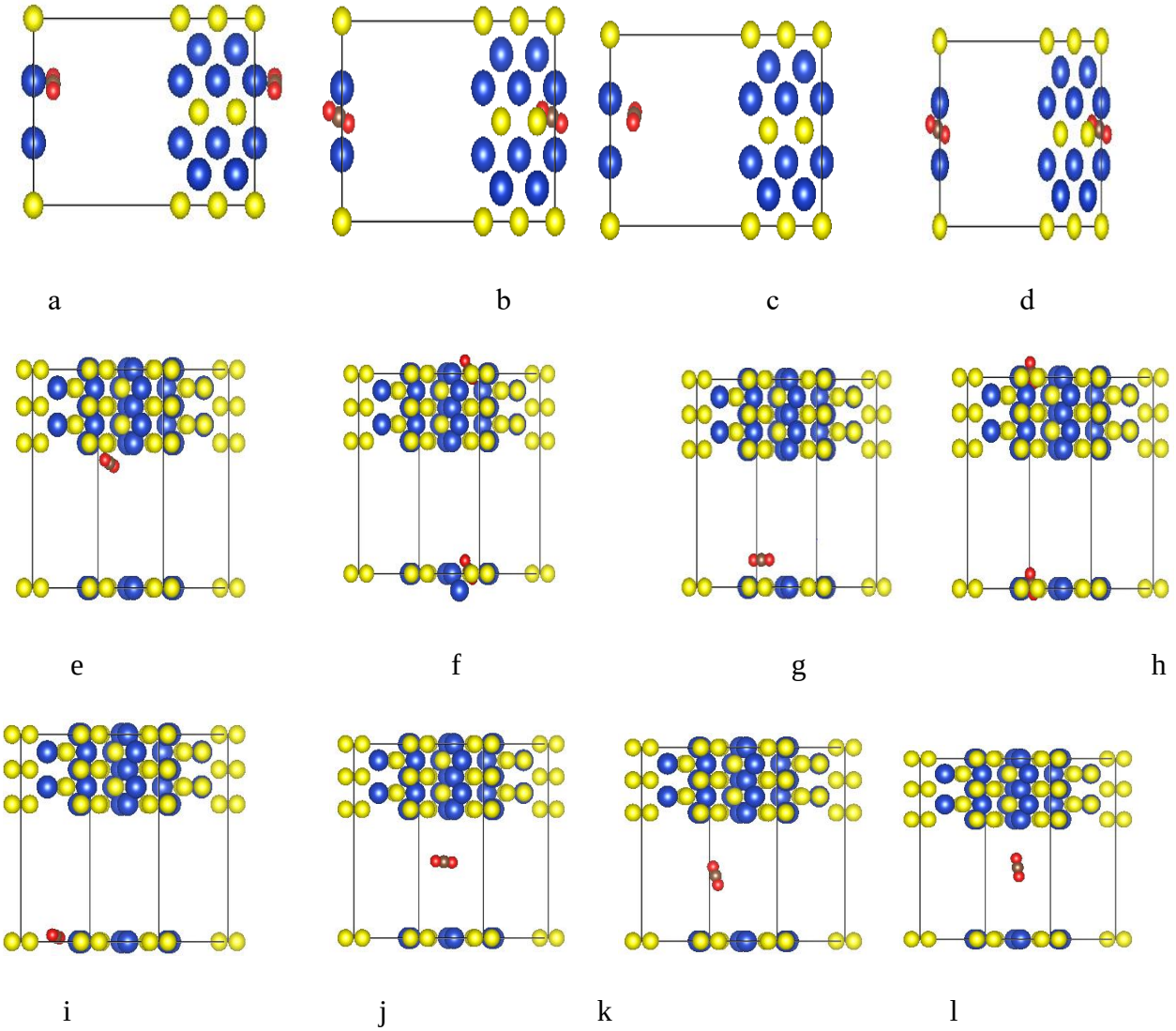

Figure 13 Geometry optimization plot of CO_2 adsorbed on the CuS (110) surface

(a) CO_2 parallel bonded on Copper and (b) CO_2 vertical bonded on copper (c) CO_2 parallel physo for CU (d) CO_2 vertical physo for Cu and (e) CO_2 parallel bonded on S (f) CO_2 vertical bonded on S (g) CO_2 parallel physo for S (h) CO_2 vertical physo for S (i) CO_2 horizontal for edge (j) CO_2 parallel for surface (k) CO_2 vertical for edge (l) CO_2 vertical for surface

Active site	*EComplex (Ry) CuS110 surface*	*Esurface(CuS110) (Ry)*	*Species energy(CO_2)(Ry)*	*Adsorption energy(Ry)*	*Adsorption energy(ev)*
Vertical Chemo at Cu	*-7211.71918789*	*-7109.98765236*	*-101.71722302*	*-0.01431251*	*-0.2*
Parallel Chemo at Cu	*-7211.73392037*	*-7109.98765236*	*-101.71722302*	*-0.02904499*	*-0.4*
Vertical for surface physo	*-7211.76180694*	*-7109.98765236*	*-101.71722302*	*-0.05693156*	*-0.775*
Parallel for surface physo	*-7211.76180833*	*-7109.98765236*	*-101.71722302*	*-0.05693295*	*-0.775*
Vertical for edge	*-7211.76077938*	*-7109.98765236*	*-101.71722302*	*-0.055904*	*-0.76*
Horizontal for edge	*-7211.70114266*	*-7109.98765236*	*-101.71722302*	*0.00373272*	*0.05*
Vertical physo for Cu	*-7211.66290848*	*-7109.98765236*	*-101.71722302*	*0.0419669*	*0.57*
Parallel physo for Cu	*-7211.75872293*	*-7109.98765236*	*-101.71722302*	*-0.05384755*	*-0.73*
Vertical chemo at S	*-7211.44002170*	*-7109.98765236*	*-101.71722302*	*0.26485368*	*3.6*
Parallel chemo at S	*-7211.59748585*	*-7109.98765236*	*-101.71722302*	*0.10738953*	*1.5*
Vertical physo for S	*-7211.74761595*	*-7109.98765236*	*-101.71722302*	*-0.04274057*	*-0.58*

Parallel physo for S	*-7211.75770759*	*-7109.98765236*	*-101.71722302*	*-0.05283221*	*-0.72*

Table 4 Complex (CuS (110) + adsorbate), slab CuS (110) Species energy (CO_2) and adsorption energy obtained from the DFT calculation (using MS software package)

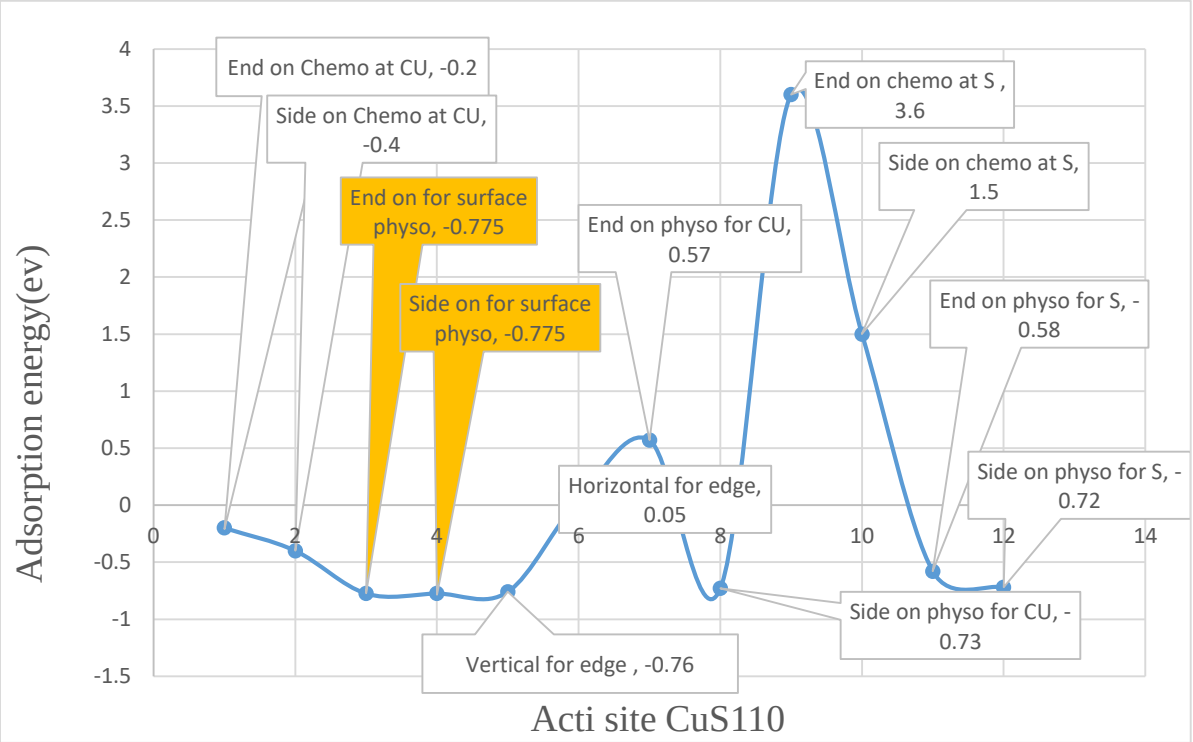

Figure 14 optimized pristine CuS(110) Adsorption energy vs Active site

Figure 14 illustrates the optimized adsorption energies of various configurations on the pristine CuS (110) surface, with the x-axis representing different adsorption sites and the y-axis indicating the adsorption energy in electronvolts (eV). Especially, configurations such as "End on for surface physo" and "Side on for surface physio" are both exhibiting significant adsorption energies of -0.775 eV, indicating their importance in the surface-adsorbate interaction.

4.5.1. Zinc doped Pristine CuS (110) Surface

To tweak the binding energy of *H species, researchers have found that blending copper with other metals, like zinc or gold, can alter the binding states of *CO species, ultimately boosting the production of C_{2+} products [81]. Yeo and colleagues found that adding zinc dopants as a co-catalyst to copper can shift the selectivity of CO_2 reduction towards producing C_2H_5OH [82]. Zinc-doped pristine copper sulfide (CuS) on the (110) surface is gaining attention in materials science and catalysis, particularly for its potential in electrochemical CO_2 reduction. Doping CuS with zinc modifies its electronic and structural properties, which can enhance its catalytic performance. The introduction of zinc alters the electronic band structure, improving conductivity and facilitating electron transfer during CO_2 reduction. Additionally, zinc doping creates new active sites, increasing surface reactivity and potentially leading to more efficient conversion of CO_2 into valuable products. The (110) surface, with its unique atomic arrangement, influences how CO_2 interacts with the catalyst, affecting reaction efficiency.

4.5.1.1. Zinc doped Pristine CuS (110) Surface one Cu replaced by one Zn

Zinc-doped pristine copper sulfide (CuS) on the (110) surface, where one copper atom is replaced by one zinc atom, presents a significant modification that can enhance the material's properties and catalytic performance, particularly in electrochemical CO_2 reduction. This substitution alters the local electronic environment and structural characteristics of the CuS lattice, potentially improving its effectiveness in various applications. The replacement of copper with zinc, which has a smaller ionic radius, may lead to changes in bond lengths and angles, creating strain in the lattice that affects surface reactivity and the adsorption energies of reactants like CO_2. Additionally, the introduction of zinc modifies the electronic band structure, enhancing conductivity and facilitating electron transfer during reactions. This doping can create new active sites, increasing the material's catalytic activity and selectivity for specific products during CO_2 reduction.

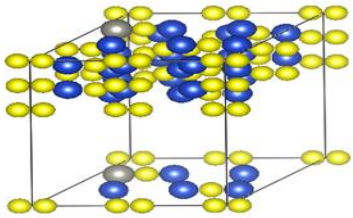

Figure 15 Zinc doped Pristine CuS (110) Surface Cu replaced by Zn

4.5.1.2. Zinc doped Pristine CuS (110) Surface one S replaced by one Zn

Zinc-doped pristine copper sulfide (CuS) on the (110) surface, where one sulfur atom is replaced by one zinc atom, introduces significant modifications that can enhance the material's structural, electronic, and catalytic properties. This substitution alters the local environment of the CuS lattice, potentially improving its performance in applications such as photocatalysis and electrochemical reactions, including CO_2 reduction. The replacement of sulfur with zinc can lead to changes in bond lengths and angles, creating distortions in the lattice that may affect the material's stability and reactivity. Additionally, zinc's different electron configuration compared to sulfur can modify the electronic band structure, enhancing conductivity and facilitating charge transfer during reactions. This doping can create new active sites, improving the adsorption of reactants like CO_2 and promoting more efficient catalytic pathways.

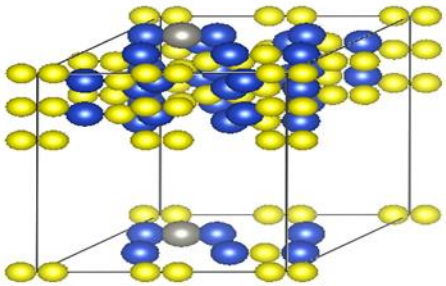

Figure 16 (a) Zinc doped Pristine CuS (110) Surface S replaced by Zn

4.5.1.3. Zn doped Pristine CuS (110) Surface Cu replaced by Zn adsorbed carbon dioxide with several active site

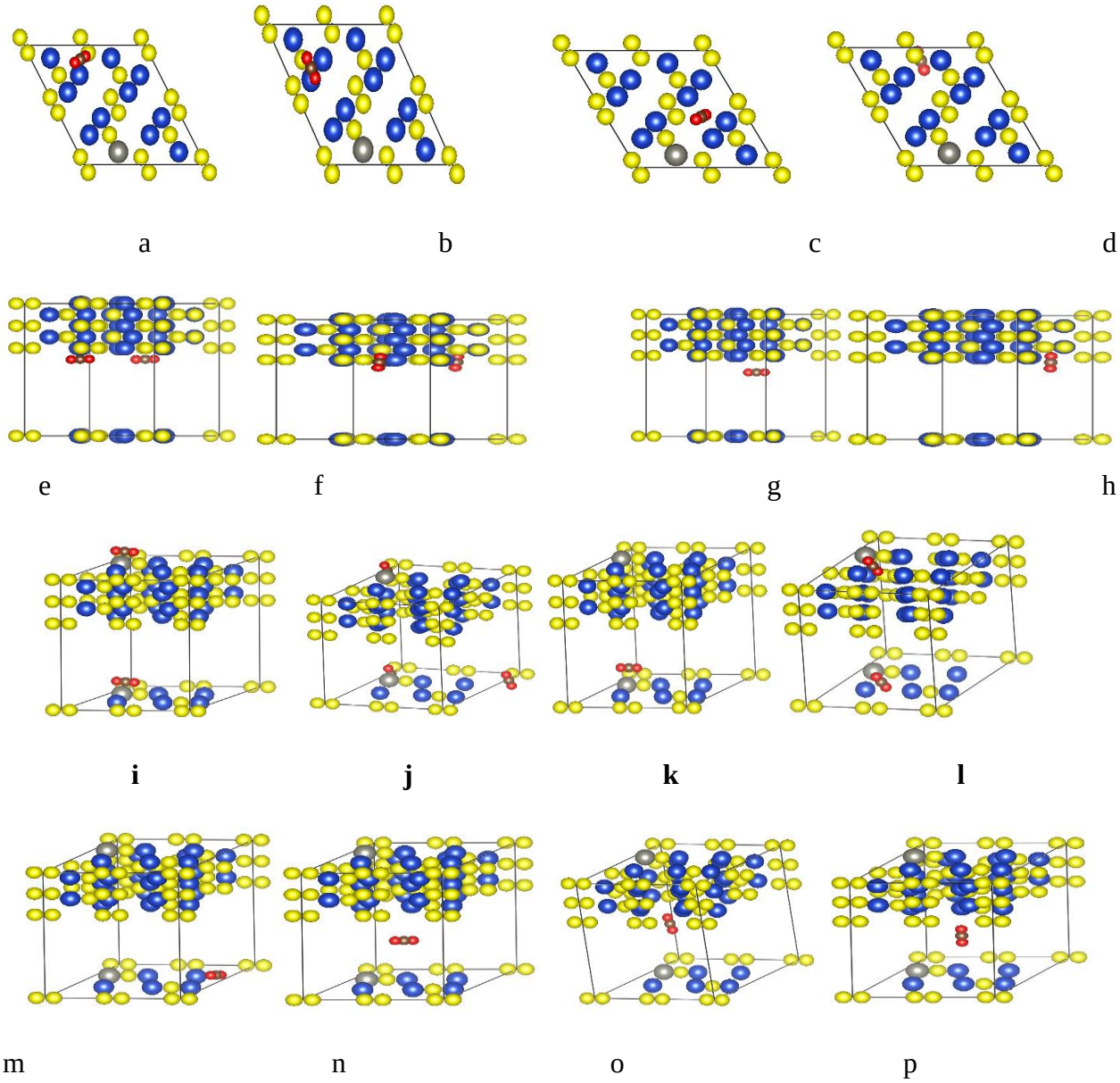

Figure 17 Geometry optimization plot of CO_2 adsorbed on Zinc doped Pristine CuS (110) Surface Cu replaced by Zn

(a) CO2 parallel bonded on Copper and (b) CO2 vertical bonded on copper (c) CO2 parallel physo for Cu (d) CO2 vertical physo for Cu (e) CO2 parallel bonded on S (f) CO2 vertical bonded on S (g) CO2 parallel physo for S (h) CO2 vertical physo for S (i) CO2 parallel bonded on Zinc and (j) CO2 vertical bonded on Zinc (k) CO2 parallel physo for Zinc (l) CO2 vertical physo for Zinc (m) CO2 horizontal for edge (n) CO2 parallel for surface (o) CO2 vertical for edge (p) CO2 vertical for surface

Active site	*EComplex (Ry)* *After 1Cu replaced by 1Zn*	*Esurface(CuS110) (Ry) after 1Cureplaced by 1Zn*	*Species energy(CO_2)(Ry)*	*Adsorption energy(Ry)*	*Adsorption energy(ev)*
Vertical Chemo at Cu	*-7460.18916774*	*-7358.54054176*	*-101.71722302*	*0.06859704*	*0.9*
Parallel Chemo at Cu	*-7460.22760037*	*-7358.54054176*	*-101.71722302*	*0.0301441*	*0.4*
Vertical for surface physo	*-7460.31163829*	*-7358.54054176*	*-101.71722302*	*-0.05387351*	*-0.7*
Parallel for surface physo	*-7460.31179484*	*-7358.54054176*	*-101.71722302*	*-0.05403006*	*-0.73*
Vertical for edge	*-7460.31090720*	*-7358.54054176*	*-101.71722302*	*-0.05314242*	*-0.72*
Horizontal for edge	*-7460.29774685*	*-7358.54054176*	*-101.71722302*	*-0.03998207*	*-0.54*
Vertical physo for Cu	*-7460.30723424*	*-7358.54054176*	*-101.71722302*	*-0.04946946*	*-0.67*
Parallel physo for Cu	*-7460.29878380*	*-7358.54054176*	*-101.71722302*	*-0.04101902*	*-0.56*
Vertical chemo at S	*-7460.01625462*	*-7358.54054176*	*-101.71722302*	*0.24151016*	*3.3*
Parallel chemo at S	*-7459.99590208*	*-7358.54054176*	*-101.71722302*	*0.2618627*	*3.56*
Vertical physo for S	*-7460.24057612*	*-7358.54054176*	*-101.71722302*	*0.01718866*	*0.23*
Parallel physo for S	*-7460.30852332*	*-7358.54054176*	*-101.71722302*	*-0.05075854*	*-0.69*
Vertical chemo at Zn	*-7460.19672817*	*-7358.54054176*	*-101.71722302*	*0.06103661*	*0.83*
Parallel chemo at Zn	*-7460.11668955*	*-7358.54054176*	*-101.71722302*	*0.14107523*	*1.9*
Vertical physo for Zn	*-7460.26805641*	*-7358.54054176*	*-101.71722302*	*-0.01029163*	*-0.14*

Parallel physo for Zn	*-7460.29852893*	*-7358.54054176*	*-101.71722302*	*-0.04076415*	*-0.55*

Table 5 Zn dopedCuS110 one Cu replaced by one Zn Complex (CuS (110) + adsorbate), slab CuS (110) Species energy(CO_2) and adsorption energy obtained from the DFT calculation (using MS software package)

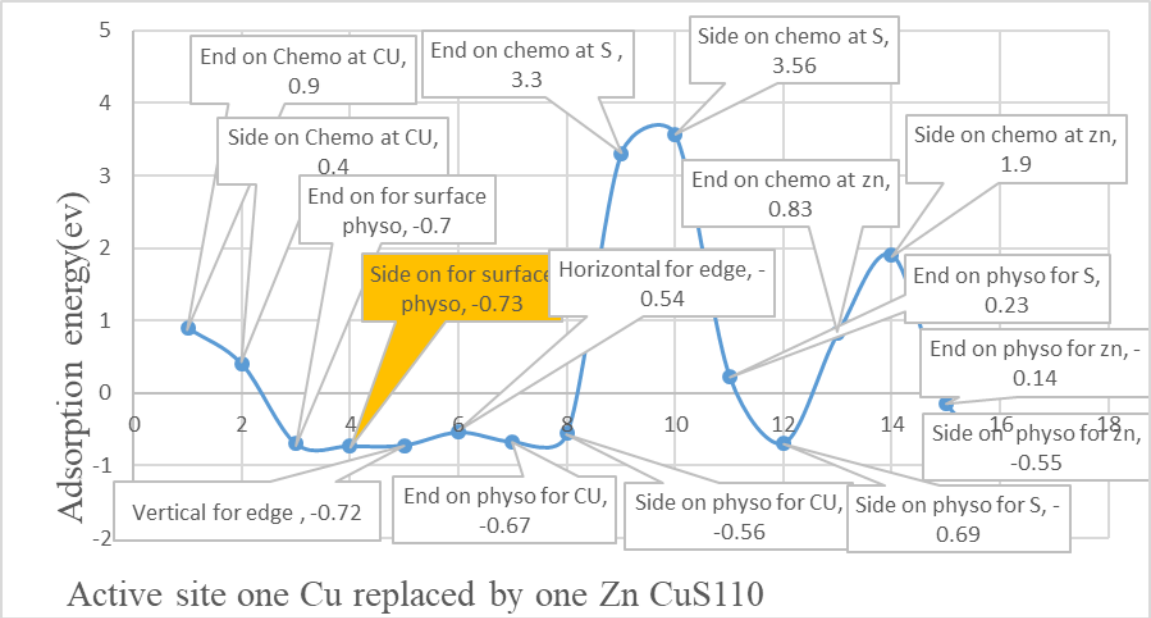

Figure 18 optimized Zn doped one Cu replaced by one Zn pristine CuS(110) Adsorption energy vs one Cu by one Zn CuS(110) surface Active site

figure 18 illustrates the adsorption energies of various configurations for a zinc-doped pristine CuS (110) surface, where one copper atom is replaced by zinc. The x-axis represents different adsorption sites, while the y-axis indicates the adsorption energy in electronvolts (eV). Notably, configurations such as "End on for surface physio", vertical for edge and "Side on for Surface physo" are , with the former exhibiting a favorable adsorption energy of -0.7ev, -0.72ev and -0.73 eV respectively, signing a strong interaction between the adsorbate and the surface.

4.5.1.4. Zn doped Pristine CuS (110) Surface S replaced by Zn adsorbed carbon dioxide with several active site

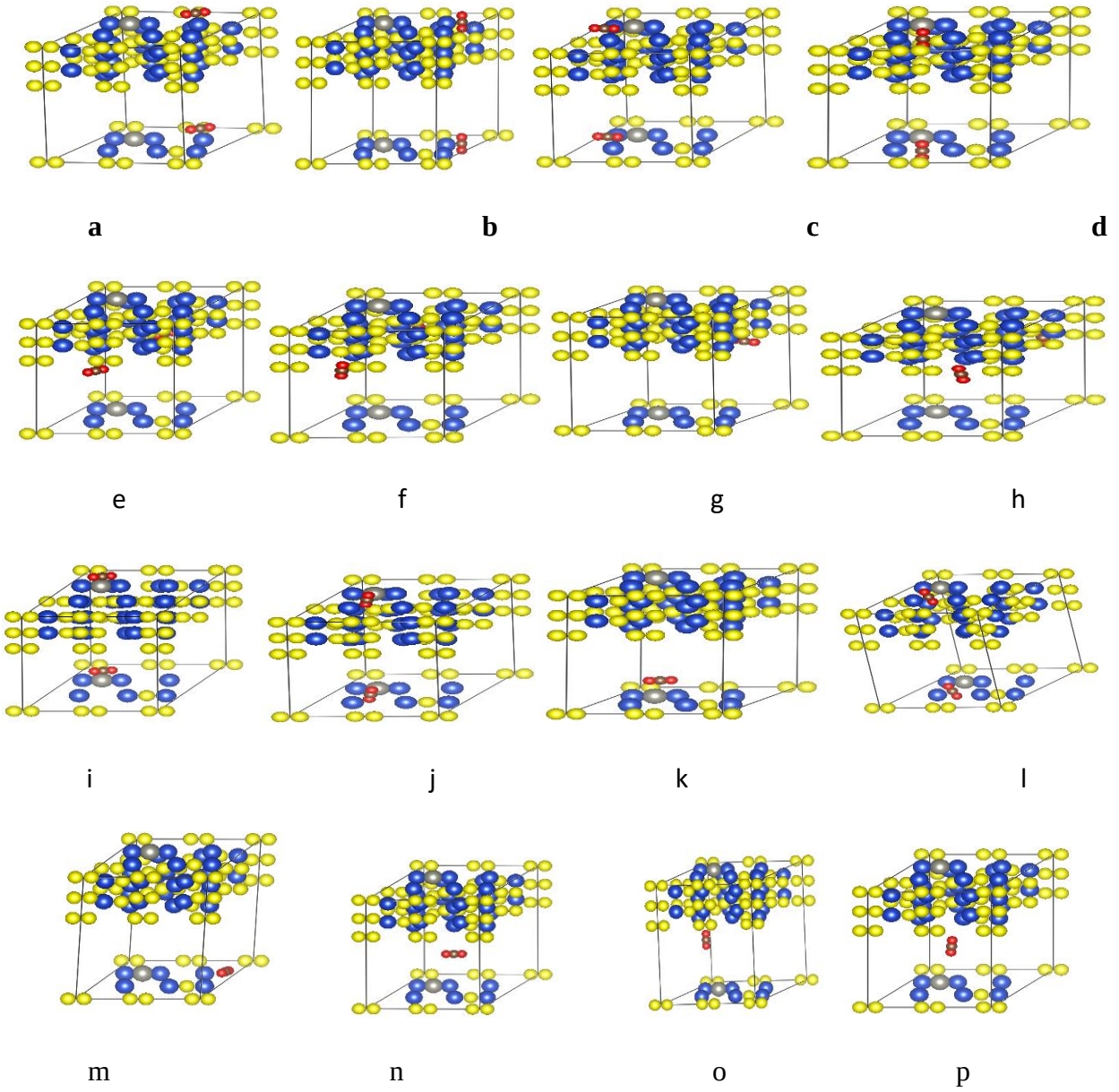

Figure 19 Geometry optimization plot of CO_2 adsorbed on Zinc doped Pristine CuS (110) Surface S replaced by Zn

(a) CO2 parallel bonded on Copper and (b) CO2 vertical bonded on copper (c) CO2 parallel physo for Cu (d) CO2 vertical physo for Cu (e) CO2 parallel bonded on S (f) CO2 vertical bonded on S (g) CO2 parallel physo for S (h) CO2 vertical physo for S (i) CO2 parallel bonded on Zinc and (j) CO2 vertical bonded on Zinc (k) CO2 parallel physo for Zinc (l) CO2 vertical physo for Zinc (m) CO2 horizontal for edge (n) CO2 parallel for surface (o) CO2 vertical for edge (p) CO2 vertical for surface

Active site	*EComplex (Ry) After 1S replaced by 1Zn*	*Esurface(CuS110) (Ry) after 1Sreplaced by 1Zn*	*Species energy(CO_2)(ev)*	*Adsorption energy(Ry)*	*Adsorption energy(ev)*
Vertical Chemo at Cu	*-7649.05263925*	*-7547.46412343*	*-101.71722302*	*0.1287072*	*1.7*
Parallel Chemo at Cu	*-7649.21165736*	*-7547.46412343*	*-101.71722302*	*-0.03031091*	*-0.4*
Vertical for surface physo	*-7649.23303214*	*-7547.46412343*	*-101.71722302*	*-0.05168569*	*-0.7*
Parallel for surface physo	*-7649.23520149*	*-7547.46412343*	*-101.71722302*	*-0.05385504*	*-0.7*
Vertical for edge	*-7649.23442800*	*-7547.46412343*	*-101.71722302*	*-0.05308155*	*-0.7*
Horizontal for edge	*-7649.23358610*	*-7547.46412343*	*-101.71722302*	*-0.05223965*	*-0.7*
Vertical physo for Cu	*-7649.22611076*	*-7547.46412343*	*-101.71722302*	*-0.04476431*	*-0.6*
Parallel physo for Cu	*-7649.19958319*	*-7547.46412343*	*-101.71722302*	*-0.01823674*	*-0.24*
Vertical chemo at S	*-7649.04979369*	*-7547.46412343*	*-101.71722302*	*0.13155276*	*1.8*
Parallel chemo at S	*-7648.91227106*	*-7547.46412343*	*-101.71722302*	*0.26907539*	*3.7*
Vertical physo for S	*-7649.22752273*	*-7547.46412343*	*-101.71722302*	*-0.04617628*	*-0.63*
Parallel physo for S	*-7649.18099231*	*-7547.46412343*	*-101.71722302*	*0.00035414*	*0.0048*

Vertical chemo at Zn	*-7649.13240581*	*-7547.46412343*	*-101.71722302*	*0.04894064*	*0.66*
Parallel chemo at Zn	*-7649.11817249*	*-7547.46412343*	*-101.71722302*	*0.06317396*	*0.86*
Vertical physo for Zn	*-7649.19956062*	*-7547.46412343*	*-101.71722302*	*-0.01821417*	*-0.25*
Parallel physo for Zn	*-7649.22397647*	*-7547.46412343*	*-101.71722302*	*-0.04263002*	*-0.58*

Table 6 Zn doped CUS110 one S replaced by one ZnComplex (CuS (110) + adsorbate), slab CuS (110) Species energy (CO_2) and adsorption energy obtained from the DFT calculation (using MS software package)

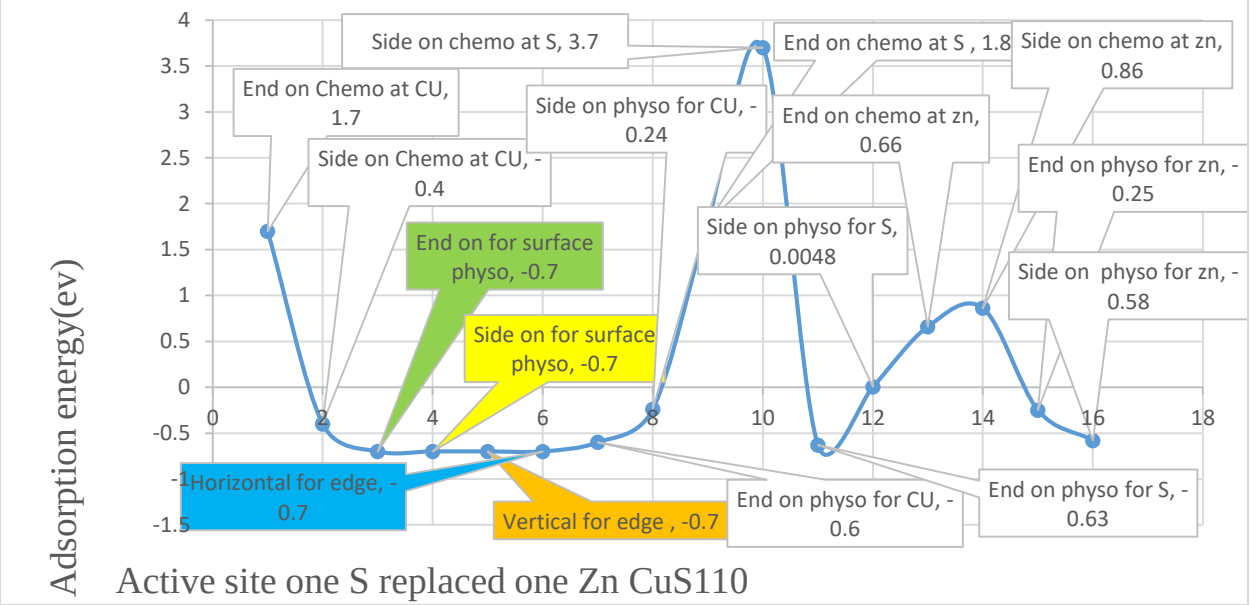

Figure 20 optimized Zn doped one S replaced by one Zn pristine CuS(110) Adsorption energy vs one S by one Zn CuS(110) surface Active site

Figure 20 discusses the adsorption energy of a zinc-doped pristine CuS (110) surface, focusing on scenarios where a sulfur (S) atom is replaced by zinc (Zn). It reveals significant fluctuations in adsorption energy (in eV), indicating that different configurations of the system possess varying stabilities. The analysis highlights various active sites, particularly the one where sulfur is replaced by zinc, suggesting that this substitution alters the surface's chemical properties and reactivity. The

graph distinguishes between chemisorption and physisorption interactions, emphasizing the structural aspects of the CuS (110) surface.

4.5.2. Cu vacancy Pristine CuS (110) Surface

The pristine copper sulfide (CuS) (110) surface exhibits unique structural and electronic properties that can be significantly influenced by the presence of copper (Cu) vacancies. These vacancies, which occur when a copper atom is missing from the lattice, can lead to local distortions in the crystal structure, altering bond lengths and angles and potentially affecting the overall stability and mechanical properties of the material. Electronically, copper vacancies create localized states in the band structure, acting as electron traps that enhance conductivity and facilitate charge carrier mobility. This modification can increase the material's reactivity, making it particularly beneficial for catalytic applications, such as CO_2 reduction, where vacancies can serve as active sites for chemical reactions, improving the adsorption of reactants and stabilizing reaction intermediates. However, while these vacancies can enhance catalytic performance, they may also impact the stability of the CuS (110) surface, increasing susceptibility to degradation under operational conditions.

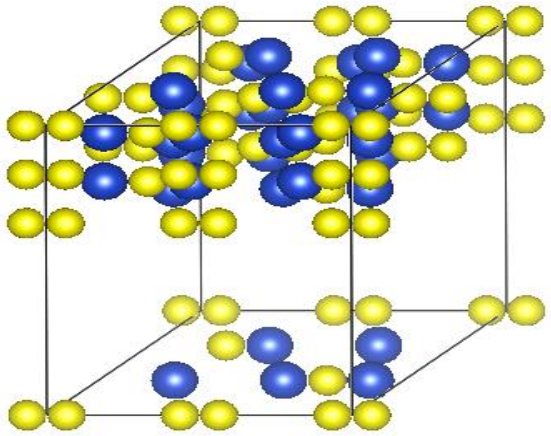

Figure 21 CU-V (V- vacancy) Pristine CuS (110) Surface

4.5.2.1. Cu vacancy Pristine CuS (110) Surface adsorbed carbon dioxide with several active site

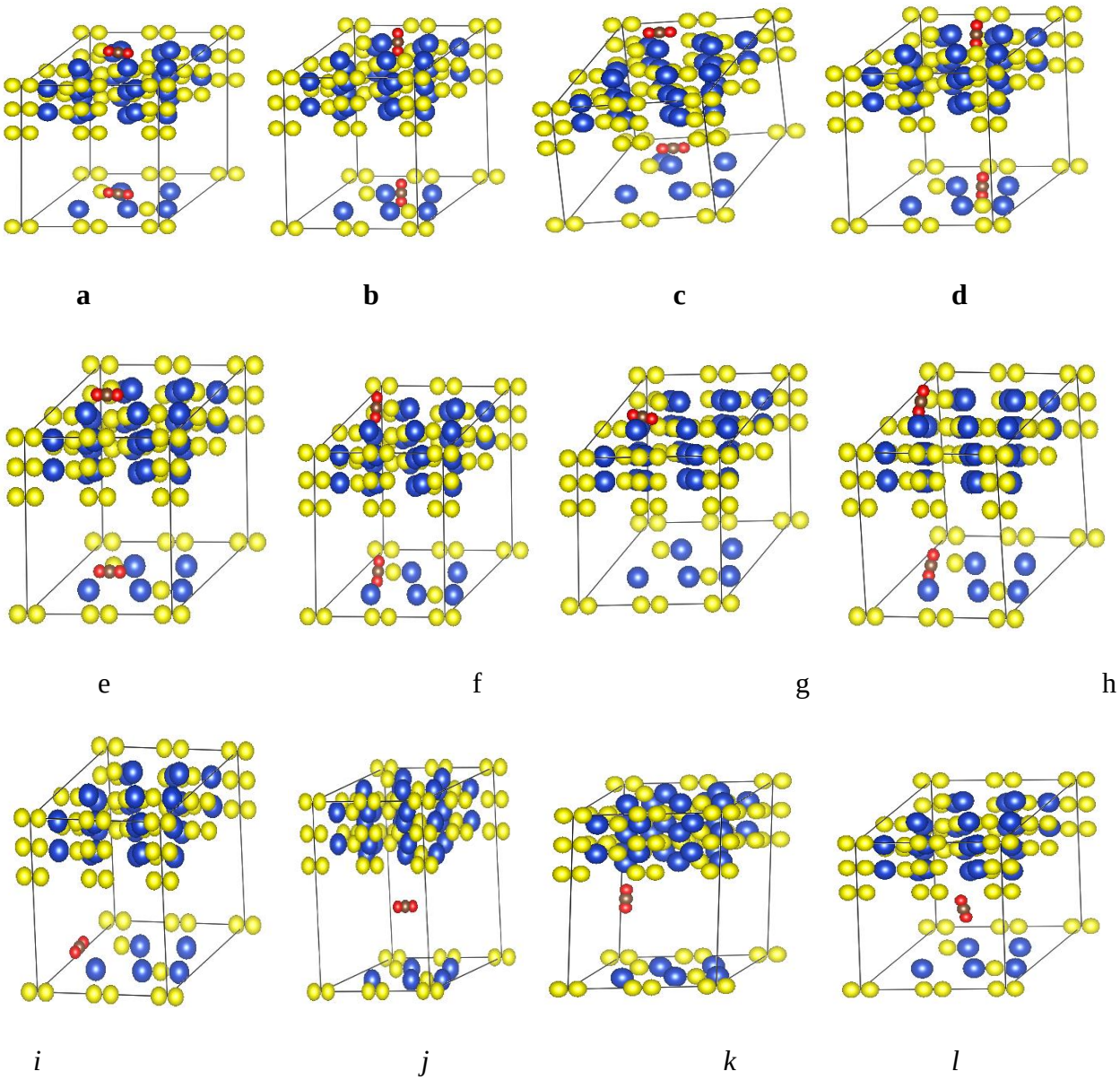

Figure 22 Geometry optimization plot of CO_2 adsorbed on one Cu – V Pristine CuS (110) Surface

(a) CO2 parallel bonded on Copper and (b) CO2 vertical bonded on copper (c) CO2 parallel physo for Cu (d) CO2 vertical physo for Cu (e) CO2 parallel bonded on S (f) CO2 vertical bonded on S (g) CO2 parallel physo for S (h) CO2 vertical physo for S (i) CO2 horizontal for edge (j) CO2 parallel for surface (k) CO2 vertical for edge (l) CO2 vertical for surface

Active site	*EComplex (Ry) 1Cu defect CuS110 surface*	*Esurface(CuS110) (Ry) 1Cu defect CuS110 surface*	*Species energy(CO_2) (Ry)*	*Adsorption energy(Ry)*	*Adsorption energy(ev)*
Vertical Chemo at Cu	*-6998.63610539*	*-6896.99091893*	*-101.71722302*	*0.07203656*	*0.98*
Parallel Chemo at Cu	*-6998.75447370*	*-6896.99091893*	*-101.71722302*	*-0.04633175*	*-0.63*
Vertical for surface physo	*-6998.76207902*	*-6896.99091893*	*-101.71722302*	*-0.05393707*	*-0.73*
Parallel for surface physo	*-6998.76213564*	*-6896.99091893*	*-101.71722302*	*-0.05399369*	*-0.73*
Vertical for edge	*-6998.76108520*	*-6896.99091893*	*-101.71722302*	*-0.05294325*	*-0.72*
Horizontal for edge	*-6998.67656404*	*-6896.99091893*	*-101.71722302*	*0.03157791*	*0.43*
Vertical physo for Cu	*-6998.69771721*	*-6896.99091893*	*-101.71722302*	*0.01042474*	*0.14*
Parallel physo for Cu	*-6998.70158890*	*-6896.99091893*	*-101.71722302*	*0.00655305*	*0.09*
Vertical chemo at S	*-6998.56830741*	*-6896.99091893*	*-101.71722302*	*0.13983454*	*1.9*
Parallel chemo at S	*-6998.67656404*	*-6896.99091893*	*-101.71722302*	*0.03157791*	*0.43*
Vertical physo for S	*-6998.71875367*	*-6896.99091893*	*-101.71722302*	*-0.01061172*	*0.14*

Parallel physo for S	*-6998.67656404*	*-6896.99091893*	*-101.71722302*	*0.03157791*	*0.43*

Table 7 one Cu defect Complex (CuS (110) + adsorbate), slab CuS (110) Species energy(CO2) and adsorption energy obtained from the DFT calculation (using MS software package)

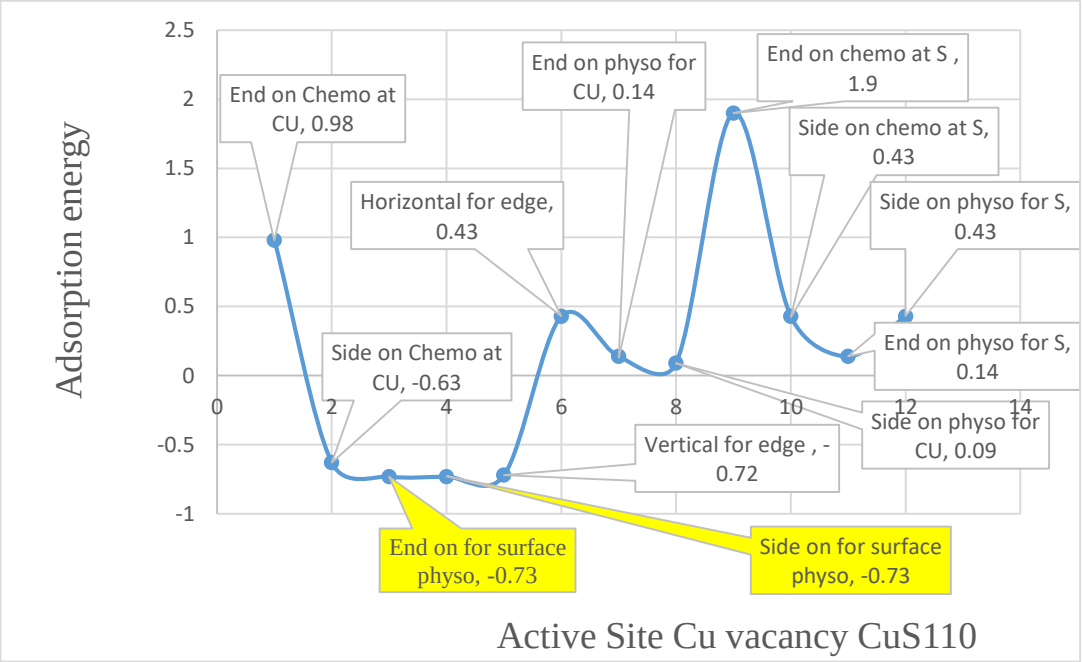

Figure 23 Cu-V (V- vacancy) Pristine CuS (110) Surface. Adsorption energy vs Cu vacancy CuS(110)surface active site

Figure 23 explores the adsorption energy of a Cu-V (vacancy) pristine CuS (110) surface, highlighting the impact of a copper (Cu) vacancy on adsorption characteristics. The graph illustrates variations in adsorption energy (in eV) for different configurations, indicating that the presence of a vacancy significantly influences the stability of the surface. Key observations include the distinction between chemisorption and physisorption interactions, with several configurations listed, such as "End on" and "Side on" for both Cu and S atoms. The highlighted active site, which features a vacancy at the Cu site, shows a notably negative adsorption energy of -0.73 eV, suggesting that this configuration is energetically favorable and enhances adsorption.

Table 8 Comparing results of adsorption energy of CO_2 in different catalytic surface

Surface	*Adsorption energy(ev)*	*Reference*
CuS(110)	*-0.775*	This work
Cu vacancy CuS(110)	*-0.73*	This work
Zn dopedCuS110	*-0.73*	This work
Ni(110)	-0.52	[83]
Fe(110)	-0.48	[84]
Pt(111)	*-0.027*	[83]
Oxygen vacancy TiO2(110)	*-0.377*	[85]
Au(100)	*-0.038*	[86]

From table 8 showed that adsorption energy of Carbon dioxide adsorbed on different catalyst at different surface such as CuS (110), Cu vacancy CuS(110),Zn dopedCuS110,Ni(110),Fe(110),Pt(111) ,Oxygen vacancy TiO2(110) and Au(100). The adsorption energy is -0.775eV, -0.73eV, -0.73eV, -0.52eV, -0.48eV, -0.027eV, -0.377eV and -0.038eV respectively. In CuS (110) surface, adsorption energy is smaller than the other surfaces hence easy reaction occurred than Ni(110),Fe(110),Pt(111) ,Oxygen vacancy TiO2(110) and Au(100). Our calculation indicate that CuS (110) catalysis is more energetically favorable for the CO2 Reduction than Ni(110), Fe(110),Pt(111) ,Oxygen vacancy TiO2(110) and Au(100) surface catalysts. This result showed that CuS 110 surface highly selective for CO2 reduction.

CHAPTER FIVE

5.Conclusion and Recommendation

In conclusion, this study successfully demonstrates that the catalytic performance of copper sulfide (CuS) for the electrochemical reduction of carbon dioxide (CO_2) into C_{2+} products can be significantly enhanced through strategic doping, defect engineering, and facet engineering. The incorporation of zinc (Zn) as a dopant and the introduction of vacancies within the CuS structure have been shown to optimize the electronic properties and active sites, leading to improved CO_2 adsorption and conversion efficiencies. Our density functional theory (DFT) calculations reveal that specific configurations, particularly the End-on and Side-on for the surface orientations on the CuS(110) surface, exhibit lower adsorption energies, indicating a more favorable reaction environment for CO_2 reduction.

The findings highlight the critical role of structural modifications in enhancing the catalytic activity and selectivity of CuS towards C_2+ products. By optimizing the active sites through doping and defect management, we have identified pathways that facilitate easier CO_2 activation and promote higher yields of desired products. Furthermore, the study underscores the importance of facet engineering in tailoring the reactivity of CuS, suggesting that specific crystal orientations can be leveraged to maximize catalytic performance.

Overall, this research contributes to the understanding of how structural and compositional changes can be employed to develop more efficient CuS-based catalysts for CO_2 conversion. The insights gained from this study pave the way for future investigations aimed at optimizing catalytic systems for sustainable energy applications, ultimately supporting efforts to mitigate CO_2 emissions and promote carbon neutrality.

Recommendation

Future research should focus on First, comprehensive Density Functional Theory (DFT) studies should be conducted to explore a wider variety of doping concentrations and configurations, including different metal dopants alongside Zn, while modeling various types of vacancy defects and their impact on electronic structures and reaction pathways. We do think it's worth exploring how chemical kinetics, which essentially governs how quickly reactions occur, influences these processes. Second in this research the band gap is not shown between valence band and conduction band in band structure of both CuS and Zn doped CuS so for future work study DFT+U when calculating band structure. Further research into this area is definitely suggested. Ultimately, conducting experiments would be a good way to confirm the findings from our theoretical models.

References

[1] M. Jitaru, “Electrochemical Carbon Dioxide Reduction - Fundamental and Applied Topics (Review),” *J. Univ. Chem. Technol. Metall.*, vol. 42, no. 4, pp. 333–344, 2007.

[2] I. S. Kwon *et al.*, “Selective electrochemical reduction of carbon dioxide to formic acid using indium – zinc bimetallic,” pp. 22879–22883, 2019, doi: 10.1039/c9ta06285h.

[3] A. R. T. Morrison *et al.*, “Modeling the Electrochemical Conversion of Carbon Dioxide to Formic Acid or Formate at Elevated Pressures,” 2019, doi: 10.1149/2.0121904jes.

[4] A. V. Rayer *et al.*, “Electrochemical carbon dioxide reduction to isopropanol using novel carbonized copper metal organic framework derived electrodes,” *J. CO2 Util.*, vol. 39, no. November 2019, p. 101159, 2020, doi: 10.1016/j.jcou.2020.101159.

[5] I. Merino-garcia, J. Albo, J. Solla-gullón, V. Montiel, and A. Irabien, “Cu oxide / ZnO-based surfaces for a selective ethylene production from gas- phase CO 2 electroconversion,” *J. CO2 Util.*, vol. 31, no. March, pp. 135–142, 2019, doi: 10.1016/j.jcou.2019.03.002.

[6] and E. S. Javed Hussain, Hannes Jonsson, “Calculations of product selectivity in electrochemical CO 2 reduction,” *ACS*, 2018, doi: 10.1021/acscatal.7b03308.

[7] H. Zhou *et al.*, “Journal of Colloid and Interface Science Recent advances in different-dimension electrocatalysts for carbon dioxide reduction,” vol. 550, no. May 2018, pp. 17–47, 2019.

[8] J. Qiao, Y. Liu, F. Hong, and J. Zhang, *A review of catalysts for the electroreduction of carbon dioxide to produce low-carbon fuels*, vol. 43, no. 2. 2014. doi: 10.1039/c3cs60323g.

[9] Y. Chen *et al.*, “Recent advances in the utilization of copper sulfide compounds for electrochemical CO2 reduction,” *Nano Mater. Sci.*, vol. 2, no. 3, pp. 235–247, 2020, doi: 10.1016/j.nanoms.2019.10.006.

[10] Y. Chen *et al.*, “Nano Materials Science Recent advances in the utilization of copper sul fi de compounds for electrochemical CO 2 reduction,” no. August, 2019.

[11] D. Gao *et al.*, “Activity and Selectivity Control in CO2 Electroreduction to Multicarbon Products over CuOx Catalysts via Electrolyte Design,” *ACS Catal.*, vol. 8, no. 11, pp. 10012–10020, 2018, doi: 10.1021/acscatal.8b02587.

[12] J. Yu *et al.*, “Recent Progresses in Electrochemical Carbon Dioxide Reduction on Copper-Based Catalysts toward Multicarbon Products,” *Adv. Funct. Mater.*, vol. 31, no. 37, pp. 1–28, 2021, doi: 10.1002/adfm.202102151.

[13] D. A. Torelli *et al.*, “Nickel-Gallium-Catalyzed Electrochemical Reduction of CO2 to Highly Reduced Products at Low Overpotentials,” *ACS Catal.*, vol. 6, no. 3, pp. 2100–2104, 2016, doi: 10.1021/acscatal.5b02888.

[14] S. Dongare, N. Singh, and H. Bhunia, “Oxide-derived Cu-Zn nanoparticles supported on N-doped graphene for electrochemical reduction of CO2 to ethanol,” *Appl. Surf. Sci.*, vol. 556, no. January, p. 149790, 2021, doi: 10.1016/j.apsusc.2021.149790.

[15] N. Zhang, C. Gao, and Y. Xiong, “Defect engineering: A versatile tool for tuning the activation of key molecules in photocatalytic reactions,” *J. Energy Chem.*, vol. 37, pp. 43–57, 2019, doi: 10.1016/j.jechem.2018.09.010.

[16] C. H. Yang, F. Nosheen, and Z. C. Zhang, “Recent progress in structural modulation of metal nanomaterials for electrocatalytic CO2 reduction,” *Rare Met.*, vol. 40, no. 6, pp. 1412–1430, 2021, doi: 10.1007/s12598-020-01600-4.

[17] S. Nitopi *et al.*, “Progress and Perspectives of Electrochemical CO2 Reduction on Copper in Aqueous Electrolyte,” *Chem. Rev.*, vol. 119, no. 12, pp. 7610–7672, 2019, doi: 10.1021/acs.chemrev.8b00705.

[18] Z. Yin, G. T. R. Palmore, and S. Sun, “Electrochemical Reduction of CO 2 Catalyzed by Metal Nanocatalysts,” *Trends Chem.*, vol. 1, no. 8, pp. 739–750, 2019, doi: 10.1016/j.trechm.2019.05.004.

[19] D. Higgins *et al.*, “Guiding Electrochemical Carbon Dioxide Reduction toward Carbonyls Using Copper Silver Thin Films with Interphase Miscibility,” *ACS Energy Lett.*, vol. 3, no. 12,

pp. 2947–2955, 2018, doi: 10.1021/acsenergylett.8b01736.

[20] X. Zhang, S. X. Guo, K. A. Gandionco, A. M. Bond, and J. Zhang, “Electrocatalytic carbon dioxide reduction: from fundamental principles to catalyst design,” *Mater. Today Adv.*, vol. 7, p. 100074, 2020, doi: 10.1016/j.mtadv.2020.100074.

[21] C. Long, X. Li, J. Guo, Y. Shi, S. Liu, and Z. Tang, “Electrochemical Reduction of CO2 over Heterogeneous Catalysts in Aqueous Solution: Recent Progress and Perspectives,” *Small Methods*, vol. 3, no. 3, pp. 1–20, 2019, doi: 10.1002/smtd.201800369.

[22] C. Cui, H. Wang, X. Zhu, J. Han, and Q. Ge, “A DFT study of CO2 electrochemical reduction on Pb(211) and Sn(112),” *Sci. China Chem.*, vol. 58, no. 4, pp. 607–613, 2015, doi: 10.1007/s11426-015-5323-z.

[23] M. Jitaru, “Electrochemical carbon dioxide reduction - Fundamental and applied topics,” no. January 2007, 2015.

[24] J. Wu, Y. Huang, W. Ye, and Y. Li, “CO 2 Reduction : From the Electrochemical to Photochemical Approach,” vol. 1700194, pp. 1–29, 2017, doi: 10.1002/advs.201700194.

[25] Z. Jiang, T. Xiao, V. L. Kuznetsov, and P. P. Edwards, “Turning carbon dioxide into fuel,” no. June, 2010, doi: 10.1098/rsta.2010.0119.

[26] L. Wu, L. Wu, C. Guo, Y. Guan, H. Wang, and J. Lu, “Progress in Electroreduction of CO2 to Form Various Fuels Based on Zn Catalysts,” *Processes*, vol. 11, no. 4, 2023, doi: 10.3390/pr11041039.

[27] P. Zhu and H. Wang, “Structural evolution of oxide-/hydroxide-derived copper electrodes accounts for the enhanced C2+ product selectivity during electrochemical CO2 reduction,” *Sci. Bull.*, vol. 65, no. 12, pp. 977–979, 2020, doi: 10.1016/j.scib.2020.03.030.

[28] M. Ebaid, K. Jiang, Z. Zhang, W. S. Drisdell, A. T. Bell, and J. K. Cooper, “Production of C2/C3Oxygenates from Planar Copper Nitride-Derived Mesoporous Copper via Electrochemical Reduction of CO2,” *Chem. Mater.*, vol. 32, no. 7, pp. 3304–3311, 2020, doi: 10.1021/acs.chemmater.0c00761.

[29] H. Mistry, A. S. Varela, S. Kühl, P. Strasser, and B. R. Cuenya, “Nanostructured electrocatalysts with tunable activity and selectivity,” *Nat. Rev. Mater.*, vol. 1, 2016, doi: 10.1038/natrevmats.2016.9.

[30] S. Balu, A. Hanan, H. Venkatesvaran, S. W. Chen, T. C. K. Yang, and M. Khalid, “Recent Progress in Surface-Defect Engineering Strategies for Electrocatalysts toward Electrochemical CO2 Reduction: A Review,” *Catalysts*, vol. 13, no. 2, pp. 1–37, 2023, doi: 10.3390/catal13020393.

[31] M. Bernal *et al.*, “CO2 electroreduction on copper-cobalt nanoparticles: Size and composition effect,” *Nano Energy*, vol. 53, pp. 27–36, 2018, doi: 10.1016/j.nanoen.2018.08.027.

[32] D. Kim, J. Resasco, Y. Yu, A. M. Asiri, and P. Yang, “Synergistic geometric and electronic effects for electrochemical reduction of carbon dioxide using gold-copper bimetallic nanoparticles,” *Nat. Commun.*, vol. 5, no. May, pp. 1–8, 2014, doi: 10.1038/ncomms5948.

[33] J. Huang, M. Mensi, E. Oveisi, V. Mantella, and R. Buonsanti, “Structural Sensitivities in Bimetallic Catalysts for Electrochemical CO2 Reduction Revealed by Ag-Cu Nanodimers,” *J. Am. Chem. Soc.*, vol. 141, no. 6, pp. 2490–2499, 2019, doi: 10.1021/jacs.8b12381.

[34] X. Jiang, N. Koizumi, X. Guo, and C. Song, “Bimetallic Pd-Cu catalysts for selective CO2 hydrogenation to methanol,” *Appl. Catal. B Environ.*, vol. 170–171, pp. 173–185, 2015, doi: 10.1016/j.apcatb.2015.01.010.

[35] J. P. Grote *et al.*, “Screening of material libraries for electrochemical CO2 reduction catalysts – Improving selectivity of Cu by mixing with Co,” *J. Catal.*, vol. 343, pp. 248–256, 2016, doi: 10.1016/j.jcat.2016.02.026.

[36] Y. Zhou *et al.*, “Dopant-induced electron localization drives CO2 reduction to C2 hydrocarbons,” *Nat. Chem.*, vol. 10, no. 9, pp. 974–980, 2018, doi: 10.1038/s41557-018-0092-x.

[37] Z. Yin *et al.*, “Cu3n nanocubes for selective electrochemical reduction of co2 to ethylene,”

Nano Lett., pp. 8658–8663, 2019, doi: 10.1021/acs.nanolett.9b03324.

[38] Y. Mi, X. Peng, X. Liu, and J. Luo, "Selective Formation of C2 Products from Electrochemical CO2 Reduction over Cu1.8Se Nanowires," *ACS Appl. Energy Mater.*, vol. 1, no. 10, pp. 5119–5123, 2018, doi: 10.1021/acsaem.8b00744.

[39] D. Ren, Y. Deng, A. D. Handoko, C. S. Chen, S. Malkhandi, and B. S. Yeo, "Selective Electrochemical Reduction of Carbon Dioxide to Ethylene and Ethanol on Copper(I) oxide catalysts," *ACS Catal.*, vol. 5, no. 5, pp. 2814–2821, 2015, doi: 10.1021/cs502128q.

[40] J. W. Vickers, D. Alfonso, and D. R. Kauffman, "Electrochemical Carbon Dioxide Reduction at Nanostructured Gold, Copper, and Alloy Materials," *Energy Technol.*, vol. 5, no. 6, pp. 775–795, 2017, doi: 10.1002/ente.201600580.

[41] R. Reske, M. Duca, M. Oezaslan, K. J. P. Schouten, M. T. M. Koper, and P. Strasser, "Controlling catalytic selectivities during CO2 electroreduction on thin Cu metal overlayers," *J. Phys. Chem. Lett.*, vol. 4, no. 15, pp. 2410–2413, 2013, doi: 10.1021/jz401087q.

[42] W. Tang *et al.*, "The importance of surface morphology in controlling the selectivity of polycrystalline copper for CO2 electroreduction," *Phys. Chem. Chem. Phys.*, vol. 14, no. 1, pp. 76–81, 2012, doi: 10.1039/c1cp22700a.

[43] D. R. Yang *et al.*, "Importance of Au nanostructures in CO2 electrochemical reduction reaction," *Sci. Bull.*, vol. 65, no. 10, pp. 796–802, 2020, doi: 10.1016/j.scib.2020.01.015.

[44] K. J. P. Soutench, Z. Qin, E. P. Gallent, and M. T. M. Koper, "Two pathways for the formation of ethylene in CO reduction on single-crystal copper electrodes," *J. Am. Chem. Soc.*, vol. 134, no. 24, pp. 9864–9867, 2012, doi: 10.1021/ja302668n.

[45] W. Luo, X. Nie, M. J. Janik, and A. Asthagiri, "Facet Dependence of CO2 Reduction Paths on Cu Electrodes," *ACS Catal.*, vol. 6, no. 1, pp. 219–229, 2016, doi: 10.1021/acscatal.5b01967.

[46] Y. Huang, A. D. Handoko, P. Hirunsit, and B. S. Yeo, "Electrochemical Reduction of CO2

Using Copper Single-Crystal Surfaces: Effects of CO∗ Coverage on the Selective Formation of Ethylene," *ACS Catal.*, vol. 7, no. 3, pp. 1749–1756, 2017, doi: 10.1021/acscatal.6b03147.

[47] F. S. Roberts, K. P. Kuhl, and A. Nilsson, "High Selectivity for Ethylene from Carbon Dioxide Reduction over Copper Nanocube Electrocatalysts," *Angew. Chemie*, vol. 127, no. 17, pp. 5268–5271, 2015, doi: 10.1002/ange.201412214.

[48] J. H. Montoya, C. Shi, K. Chan, and J. K. Nørskov, "Theoretical insights into a CO dimerization mechanism in CO2 electroreduction," *J. Phys. Chem. Lett.*, vol. 6, no. 11, pp. 2032–2037, 2015, doi: 10.1021/acs.jpclett.5b00722.

[49] X. Nie, W. Luo, M. J. Janik, and A. Asthagiri, "Reaction mechanisms of CO 2 electrochemical reduction on Cu (1 1 1) determined with density functional theory," *J. Catal.*, vol. 312, pp. 108–122, 2014, doi: 10.1016/j.jcat.2014.01.013.

[50] W. J. Durand, A. A. Peterson, F. Studt, F. Abild-Pedersen, and J. K. Nørskov, "Structure effects on the energetics of the electrochemical reduction of CO2 by copper surfaces," *Surf. Sci.*, vol. 605, no. 15–16, pp. 1354–1359, 2011, doi: 10.1016/j.susc.2011.04.028.

[51] I. Ledezma-Yanez, E. P. Gallent, M. T. M. Koper, and F. Calle-Vallejo, "Structure-sensitive electroreduction of acetaldehyde to ethanol on copper and its mechanistic implications for CO and CO2 reduction," *Catal. Today*, vol. 262, pp. 90–94, 2016, doi: 10.1016/j.cattod.2015.09.029.

[52] A. S. Varela, M. Kroschel, T. Reier, and P. Strasser, "Controlling the selectivity of CO2 electroreduction on copper: The effect of the electrolyte concentration and the importance of the local pH," *Catal. Today*, vol. 260, pp. 8–13, 2016, doi: 10.1016/j.cattod.2015.06.009.

[53] C. W. Li, J. Ciston, and M. W. Kanan, "Electroreduction of carbon monoxide to liquid fuel on oxide-derived nanocrystalline copper," *Nature*, vol. 508, no. 7497, pp. 504–507, 2014, doi: 10.1038/nature13249.

[54] C. S. Chen, A. D. Handoko, J. H. Wan, L. Ma, D. Ren, and B. S. Yeo, “Stable and selective electrochemical reduction of carbon dioxide to ethylene on copper mesocrystals,” *Catal. Sci. Technol.*, vol. 5, no. 1, pp. 161–168, 2015, doi: 10.1039/c4cy00906a.

[55] G. L. De Gregorio, T. Burdyny, A. Loiudice, P. Iyengar, W. A. Smith, and R. Buonsanti, “Facet-Dependent Selectivity of Cu Catalysts in Electrochemical CO2 Reduction at Commercially Viable Current Densities,” *ACS Catal.*, vol. 10, no. 9, pp. 4854–4862, 2020, doi: 10.1021/acscatal.0c00297.

[56] C. Xie *et al.*, “Insight into the design of defect electrocatalysts: From electronic structure to adsorption energy,” *Mater. Today*, vol. 31, no. xx, pp. 47–68, 2019, doi: 10.1016/j.mattod.2019.05.021.

[57] Y. Shi, Z. Lyu, M. Zhao, R. Chen, Q. N. Nguyen, and Y. Xia, “Noble-Metal Nanocrystals with Controlled Shapes for Catalytic and Electrocatalytic Applications,” *Chem. Rev.*, vol. 121, no. 2, pp. 649–735, 2021, doi: 10.1021/acs.chemrev.0c00454.

[58] S. Lu *et al.*, “Crystal phase control of gold nanomaterials by wet-chemical synthesis,” *Acc. Chem. Res.*, vol. 53, no. 10, pp. 2106–2118, 2020, doi: 10.1021/acs.accounts.0c00487.

[59] C. Xie, Z. Niu, D. Kim, M. Li, and P. Yang, “Surface and Interface Control in Nanoparticle Catalysis,” *Chem. Rev.*, vol. 120, no. 2, pp. 1184–1249, 2020, doi: 10.1021/acs.chemrev.9b00220.

[60] Y. Takeuchi, “A refinement of the crystal structure of covellite , CuS,” vol. 8, no. 6, 1977.

[61] A. Soares and A. Morales-garcia, “The Stability and Structural , Electronic and Topological Properties of Covellite (001) Surfaces .,” no. July, 2016, doi: 10.1002/slct.201600422.

[62] A. L. S. Jr, E. C. Dos Santos, T. Heine, and H. A. De Abreu, “Two-dimensional crystal CuS—electronic and structural properties,” *2D Mater.*, vol. 4, no. 1, pp. 1–7, doi: 10.1088/2053-1583/aa516e.

[63] R. Gaspari, L. Manna, A. Cavalli, R. Gaspari, L. Manna, and A. Cavalli, “A theoretical investigation of the (0001) covellite surfaces,” vol. 044702, no. 0001, 2014, doi:

10.1063/1.4890374.

[64] B. R. Tagirov, A. L. Trigub, and K. O. Kvashnina, “ScienceDirect Covellite CuS as a matrix for ‘‘ invisible ” gold : X-ray spectroscopic study of the chemical state of Cu and Au in synthetic minerals,” *Geochim. Cosmochim. Acta*, vol. 191, no. August, pp. 58–69, 2016, doi: 10.1016/j.gca.2016.07.015.

[65] A. L. S. Jr, E. C. Dos Santos, T. Heine, and H. A. De Abreu, “Two-dimensional crystal CuS—electronic and structural properties,” vol. 015041.

[66] C. Cus, A. Morales-garc, A. L. Soares, E. C. Dos Santos, and H. A. De Abreu, “First-Principles Calculations and Electron Density Topological Analysis of Covellite (CuS),” no. November 2017, 2014, doi: 10.1021/jp4114706.

[67] A. Morales-garc, A. L. Soares, E. C. Dos Santos, H. A. De Abreu, and A. Duarte, “First-Principles Calculations and Electron Density Topological Analysis of Covellite (CuS),” 2014, doi: 10.1021/jp4114706.

[68] C. Dong, M. Ji, X. Yang, J. Yao, and H. Chen, “Formaldehyde Catalyzed by Hourglass Ru , Fe ,” vol. 2, doi: 10.3390/catal7010005.

[69] G. Kresse and D. Joubert, “From ultrasoft pseudopotentials to the projector augmented-wave method,” vol. 59, no. 3, pp. 11–19, 1999.

[70] P. Schwerdtfeger, “The Pseudopotential Approximation in Electronic Structure Theory,” pp. 3143–3155, 2011, doi: 10.1002/cphc.201100387.

[71] G. R. Schleder, A. C. M. Padilha, C. M. Acosta, and M. Costa, “From DFT to machine learning : recent approaches to materials science – a review From DFT to machine learning : recent approaches to materials science – a review,” *J. Phys. Mater.*, vol. 2, no. 3, p. 32001, 2019, doi: 10.1088/2515-7639/ab084b.

[72] P. Giannozzi *et al.*, “Q UANTUM ESPRESSO : a modular and open-source software project for quantum simulations of materials,” vol. 395502, 2009, doi: 10.1088/0953-8984/21/39/395502.

[73] Q.- Espresso, C. M. Dynamics, and F. M. Dynamics, “Lab 2 : Handout Quantum-Espresso : a first-principles code,” pp. 1–20, 2005.

[74] “VESTA : A Three-Dimensional Visualization System for Electronic and structural analysis,” no. June 2008, 2014, doi: 10.1107/S0021889808012016.

[75] M. Meunier, “Introduction to Materials Studio,” no. June 2012, 2016, doi: 10.1051/epjconf/20123004001.

[76] A. Kokalj, “XCrySDen-a new program for displaying crystalline structures and electron densities,” *J. Mol. Graph. Model.*, vol. 17, no. 3–4, pp. 176–179, 1999, doi: 10.1016/S1093-3263(99)00028-5.

[77] M. J. S. Spencer and G. L. Nyberg, “DFT modelling of hydrogen on CU(110)- and (111)-type clusters,” *Mol. Simul.*, vol. 28, no. 8–9, pp. 807–825, 2002, doi: 10.1080/0892702021000002502.

[78] H. J. Monkhorst and J. D. Pack, “Special points for Brillonin-zone integrations* Hendrik,” vol. 13, no. 12, pp. 5188–5192, 1976.

[79] Y. Takéuchi, Y. Kudoh, and G. Sato, “The crystal structure of covellite CuS under high pressure Up to 33 kbar,” vol. 1985, pp. 119–128, 1985.

[80] B. M. Abraham and G. Vaitheeswaran, “DFT study of the formate formation on Ni (111) surface doped by transition metals [Ni (111) -M ; M = Cu , Pd , Pt , Rh],” no. 111, 2016, doi: 10.1088/1742-6596/739/1/012082.

[81] H. Zhang *et al.*, “Computational and experimental demonstrations of one-pot tandem catalysis for electrochemical carbon dioxide reduction to methane,” *Nat. Commun.*, vol. 10, no. 1, pp. 1–9, 2019, doi: 10.1038/s41467-019-11292-9.

[82] Y. Feng *et al.*, “Laser-Prepared CuZn Alloy Catalyst for Selective Electrochemical Reduction of CO2 to Ethylene,” *Langmuir*, vol. 34, no. 45, pp. 13544–13549, 2018, doi: 10.1021/acs.langmuir.8b02837.

[83] X. Liu, L. Sun, and W. Q. Deng, “Theoretical Investigation of CO2 Adsorption and

Dissociation on Low Index Surfaces of Transition Metals," *J. Phys. Chem. C*, vol. 122, no. 15, pp. 8306–8314, 2018, doi: 10.1021/acs.jpcc.7b12660.

[84] H. Wang, X. Nie, Y. Chen, X. Guo, and C. Song, "Facet effect on CO2 adsorption, dissociation and hydrogenation over Fe catalysts: Insight from DFT," *J. CO2 Util.*, vol. 26, no. January, pp. 160–170, 2018, doi: 10.1016/j.jcou.2018.05.003.

[85] Y. Bo and C. Gao, "Recent advances in engineering active sites for photocatalytic CO 2 reduction," pp. 12196–12209, 2020, doi: 10.1039/d0nr02596h.

[86] T. Cheng, Y. Huang, H. Xiao, and W. A. Goddard, "Predicted Structures of the Active Sites Responsible for the Improved Reduction of Carbon Dioxide by Gold Nanoparticles," *J. Phys. Chem. Lett.*, vol. 8, no. 14, pp. 3317–3320, 2017, doi: 10.1021/acs.jpclett.7b01335.